

UNIVERSIDAD SAN FRANCISCO DE QUITO

USFQ

Colegio de Ciencias e Ingenierías

**Comparative Analysis between Native, Stenotic and
Mechanical Aortic Valves using FSI (Fluid Structure
Interaction) Module**

Proyecto de Investigación

Mauro David Espinosa Segarra

José Diego Masache Cevallos

Ingeniería Mecánica

Proyecto de Titulación presentado como requisito para la obtención del título de

Ingeniero Mecánico

Quito, 24 de mayo de 2017

UNIVERSIDAD SAN FRANCISCO DE QUITO
USFQ

Colegio de Ciencias e Ingenierías

Hoja de Calificación de Trabajo de Titulación

**Comparative Analysis between Native, Stenotic and Mechanical Aortic
Valves using FSI (Fluid Structure Interaction) Module**

Mauro David Espinosa Segarra
José Diego Masache Cevallos

Calificación:

Nombre del profesor, Título académico

David Escudero, Ph.D.

Firma del Profesor

Quito, 24 de mayo de 2017

Derechos de Autor

Por medio del presente documento certifico que he leído todas las Políticas y Manuales de la Universidad San Francisco de Quito USFQ, incluyendo la Política de Propiedad Intelectual USFQ, y estoy de acuerdo con su contenido, por lo que los derechos de propiedad intelectual del presente trabajo quedan sujetos a lo dispuesto en esas Políticas.

Asimismo, autorizo a la USFQ para que realice la digitalización y publicación de este trabajo en el repositorio virtual, de conformidad a lo dispuesto en el Art. 144 de la Ley Orgánica de Educación Superior.

Firma del estudiante: _____

Nombres y apellidos: Mauro David Espinosa Segarra

Código: 00107099

Cédula de Identidad: 1715889356

Firma del estudiante: _____

Nombres y apellidos: José Diego Masache Cevallos

Código: 00107931

Cédula de Identidad: 1717656720

Lugar y fecha: Quito, 24 de mayo de 2017

INSCRIPTION

To God for guiding my path and for giving me strength in difficult times to continue.

To David Escudero, Ph.D. Because he guided and supported us with his knowledge and experience, so that this work can be carried out successfully.

To Maurito, my thesis partner, since he was the complement to finish this work and also was a great support throughout the career and this study.

To Jose, my thesis partner, since he has been a loyal and hard-working companion during all the projects that we have made including this investigation.

To our parents who made it possible for me to finish my career, because they knew how to guide me throughout my studies and I always had their unconditional support.

To our teachers, because they knew how to transmit their knowledge in an impeccable way.

To our university that was the center where we acquired several knowledge that has been reflected in this work.

To our friends because they always give us their words of encouragement and their unconditional friendship.

José and Mauro

RESUMEN

La estenosis es una valvulopatía que afecta el funcionamiento correcto de la válvula aórtica hasta el punto de que un paciente con este problema debe someterse a un procedimiento quirúrgico de cambio de válvula donde su válvula estenótica es reemplazada por una válvula mecánica. Este estudio muestra un análisis comparativo para tres tipos de válvulas aórticas (nativa saludable, estenótica y prótesis mecánica) donde se evalúa el comportamiento de estas en cuanto a la presión, velocidad sanguínea y esfuerzos localizados en las valvas. Para esto se utiliza un módulo FSI del software COMSOL Multiphysics para simulaciones en 2D. En cuanto a los resultados de presión, las curvas obtenidas después de la simulación muestran un comportamiento fisiológico similar a la presión arterial del cuerpo humano. Para la válvula nativa y la prótesis mecánica se arrojaron valores de 80 a 120 mmHg, mientras que en el caso de la válvula estenótica se tiene valores de 70 a 110 mmHg. Del mismo modo, en cuanto a las velocidades del flujo sanguíneo los valores máximos se presentan en la válvula estenótica y son cercanos a $2.6 \left[\frac{m}{s} \right]$, mientras que para la válvula nativa y la mecánica los valores no superan $1.5 \left[\frac{m}{s} \right]$. Para los esfuerzos de Von Mises el estudio muestra valores de tensión y compresión localizados en la pared arterial donde las valvas se encuentran fijadas. El rango de valores obtenido es mayor para la válvula estenótica debido a la presencia de calcificaciones al compararla con la válvula nativa. Finalmente, todos estos resultados sirven como contribución a la limitada información disponible acerca de este tópico en el Ecuador.

Palabras claves: válvula aórtica, endógena, estenosis, valvulopatía, incompresible, esfuerzo de Von Mises, gradiente, simulación, hemodinámica.

ABSTRACT

Stenosis is a valvulopathy that affects the correct functioning of an aortic valve to the point that a person with this disease must undergo a surgical procedure where his or her SAV is replaced by a MAV. This study shows a comparative analysis for the three types of AV's (NAV, SAV and MAV) in such a way to analyze the range of values for pressures, velocities and stresses. For that, the module FSI of software COMSOL Multiphysics have been used in order to perform 2D simulations. Regarding the pressure, the results showed that the curves obtained after the simulations has the physiological behavior of the human body arterial pressure. For the NAV and MAV it corresponds to values from 80 to 120 mmHg and for the SAV it has values from 70 to 110 mmHg. In the same way, the maximum value for the velocity of the blood flow for the SAV is $2.6 \left[\frac{m}{s} \right]$ and the velocities for NAV and MAV are below $1.5 \left[\frac{m}{s} \right]$. For the Von Mises stresses, the study shows values for tension and compression located at the arterial wall where the NAV and SAV are fixed. The range of values obtained is higher for the SAV than for the NAV due to the calcifications present in the SAV. Finally, this results serve as a contribution to the limited information available about this topic in Ecuador.

Key words: aortic valve, native, stenosis, valvulopathy, incompressible, Von Mises stress, gradient, simulation, hemodynamics.

TABLE OF CONTENTS

1. INTRODUCTION	13
1.1. Motivation.....	13
1.2. General Objective.	14
1.3. Specific Objectives.	14
2. LITERATURE REVIEW	15
2.1. AR Geometry Studies.	15
2.2. Models using ALE method for FSI Analysis.	18
3. THEORETICAL FRAMEWORK AND MODEL DEFINITION.....	21
3.1. How the AV Works.	21
3.2. Stenosis on AV	23
3.3. Mechanical AV Function.....	24
3.4. Theory for Fluid Interface.	27
3.5. Model Description.	29
4. RESULTS	40
4.1. Pressure.....	40
4.2. Velocity.....	43
4.3. Von Mises Stresses.....	48
5. CONCLUSIONS.....	51
6. RECOMMENDATIONS	53
7. FUTURE WORK.....	54
8. REFERENCES	55

LIST OF TABLES

Table 1. Classification of the AR used in the study, regarding the age of the donor (Swanson & Clark, 1974).....	15
Table 2. Material properties for a 2D flow study on a MAV (Yeh et al., 2014).	19
Table 3. Different St. Jude Medical MAVs regarding its size (St. Jude Medical, 2013)	27
Table 4. Parameters for each material.....	30
Table 5. General geometry measures.....	34
Table 6. Thickness of the aortic valves.....	35
Table 7. Specifications of each mesh used for the study	38

LIST OF FIGURES

Figure 1. Mean measures (in inches) of the AV casts (Swanson & Clark, 1974)	16
Figure 2. Two 3D different model of AR. a) 5 series AR geometry b) 8 series AR geometry (Burken et al., 2011)	17
Figure 3. 2D geometry of the mitral valves used for the FSI model (Azrul et al., 2011)	18
Figure 4. Anatomy of the AR (Weinberg, Schoen, & Mofrad, 2009)	21
Figure 5. AV (enclosed in a circle) function inside the cardiac cycle. (A) describes the diastolic phase where the left ventricle fills with blood. (B) describes the systolic phase where the AV opens (Texas Heart Institute, 2015)	22
Figure 6. Cardiac cycle specifications (Hall & Guyton, 2007)	23
Figure 7. (Left) NAV vs (Right) moderate SAV (Baumgartner et al., 2009).....	23
Figure 8. Effective area of blood flow in mild, moderate and severe cases of SAV (Weinberg et al., 2009)	24
Figure 9. St. Jude Medical Regent Heart Valve (St. Jude Medical, 2013).....	25
Figure 10. Parts of the MAV (St. Jude Medical, 2013).....	26
Figure 11. Normal arterial pressure function.....	32
Figure 12. Arterial pressure function used for the SAV	33
Figure 13. Initial left ventricular volume used in the study.....	34
Figure 14. NAV geometry which each section described	35
Figure 15. SAV geometry.....	36
Figure 16. MAV geometry	36
Figure 17. Initial blood velocity during the systolic phase.....	39
Figure 18. Pressure for NAV	40

Figure 19. Pressure for SAV	41
Figure 20. Pressure for MAV	42
Figure 21. Quantitative results for the three cases of AV's.....	43
Figure 22. Velocity for NAV.....	44
Figure 23. Velocity for SAV	45
Figure 24. Velocity for MAV	46
Figure 25. Velocity for AV's.....	47
Figure 26. Von Mises stresses for NAV.....	48
Figure 27. Von Mises stresses for SAV.....	49
Figure 28. Von Mises stresses in tension for AV's.	49
Figure 29. Von Mises stresses in compression for AV's.....	50

NOMENCLATURE

Abbreviations

AR: Aortic Root

AV: Aortic valve

MAV: Mechanical Aortic Valve

NAV: Native Aortic Valve

SAV: Stenotic Aortic Valve

Notation

c : Sound velocity

C_p : Specific heat capacity at constant pressure $\left[\frac{J}{kg K}\right]$

E : Young Modulus [MPa]

F : Volume force vector $\left[\frac{N}{m^3}\right]$

L : Length [m]

M_a : Mach number

p : Pressure [Pa]

Q : Heat sources $\left[\frac{W}{m^3}\right]$

S : Strain rate tensor

t : Time [s]

T : Absolute temperature [K]

u : Velocity $\left[\frac{m}{s}\right]$

ν : Poisson modulus.

V : Volume $[m^3]$

Greek letters

ρ : Density $\left[\frac{kg}{m^3}\right]$

μ : Dynamic viscosity [Pa·s]

τ : Viscous stress tensor [Pa]

λ : Lamé Parameters

1. INTRODUCTION

1.1. Motivation

The aortic valve is an accurate and important structure in the functioning of the heart; nonetheless, with the past of time it could present diseases that affect severely the hemodynamics at the AR. One of its complications is stenosis. This valvulopathy occurs when there is a narrowing in the valves of the AV caused by the accumulation of calcifications in its walls so the blood flow decreases. When this occurs, surgical intervention or cardiac catheterization is necessary, in most cases. Because of the complexity that an operation of this kind could require, there are several risks to the patient, as well as investment of time and money. For this reason, there has been a need to carry out an investigation regarding AVs and the blood flow that passes through them in the stenotic case. Firstly, to achieve this there must be a comparative study that involves an analysis of blood flow through a healthy AV, so the study could present a considerable difference in the change of AV hemodynamics. Also, the study must show a solution to the stenotic case, which is the implantation of a mechanical AV and how the blood flow behaves with this prosthesis, which must be similar to the flow presented with the healthy AV, representing a normalization of blood flow through the AR.

In Ecuador, there are no studies that involves medical engineering analysis of hemodynamics applied on an AV. However, the cardiac surgery involving the AV is a common practice. For example, there has been a study between 2009 and 2010 in Hospital Carlos Andrade Marín from a sample of 147 patients with a mean age of 51 years old, where 66 of them were performed valve surgery, of which 50% were cases of AV replacement (Aguirre, Ortega, & Arcos, 2015). Similarly, between 2012 and 2013 the Hospital de Especialidades de las Fuerzas Armadas made a study involving a sample of 240 patients with a mean age of 64.6 years old, in which 29.1% of total were cases of

stenosis and valve replacement on AV (Aguirre & A, 2015). These data show that cardiac surgeries involving valvulopathies and valve replacement are present in hospitals in the country, so a medical engineering study can complement these practices in order that the cardiology doctors use the model presented in this work as pre or postoperative reference from their surgeries and investigations regarding the hemodynamics located at the AR.

1.2. General Objective

- To carry out an FSI comparative analysis which presents the behavior of hemodynamics on a native, stenotic and mechanical AV using COMSOL Multiphysics software for the enrichment of medical engineering cardiology information about this topic in Ecuador.

1.3. Specific Objectives

- To perform a FSI model in COMSOL Multiphysics by applying the equations of Navier-Stokes for a 2D fluid model.
- To understand the hemodynamics different behavior between NAV, SAV and MAV.
- To determine the pressure and velocity field of the blood flow through the AR inside the cardiac cycle.
- To investigate the strength that support the valves (gates) of the AV to prevent the passage of blood flow.
- To obtain the difference of pressures that must exist in the AR between the annulus and the ascending aorta so that the valve closes automatically.
- To define the material and mechanism conditions which the MAV possesses, so the blood flow in the AR behaves similar as the NAV case.

2. LITERATURE REVIEW

In terms of literature, there have been a considerable amount of studies that concentrate on AV biomechanical properties. However, Hasan et al., mention that while significant progress has been made toward improving the design and performance of native and mechanical heart valves, “the need for better understanding and more detailed characterization of mechanical properties of native heart valve is imperative considering its geometry, hemodynamic conditions, and the behavior of the valves in response of the fluid flow” (Hasan et al., 2014).

2.1. AR Geometry Studies

First of all, there has been a study that evaluates the dimension and geometry of ARs by casting silicone rubber in several tissue models as a function of intra-aortic pressure between 0 and 120 mmHg. This helps to get an accurate idea of what the dimensions of a NAV should be in terms of the blood flow analysis (Swanson & Clark, 1974). It is worth mention that the study was separated in five series considering the size of the AR which mostly increases with the age as shown in Table 1.

Table 1. Classification of the AR used in the study, regarding the age of the donor (Swanson & Clark, 1974).

Valve Series	Age (years)	Sex
4	29	F
5	39	M
6	29	F
7	35	F
8	42	M

With the geometry data collected, Swanson and Clark made a model with significant dimensions obtained towards the study, as shown in Figure 1.

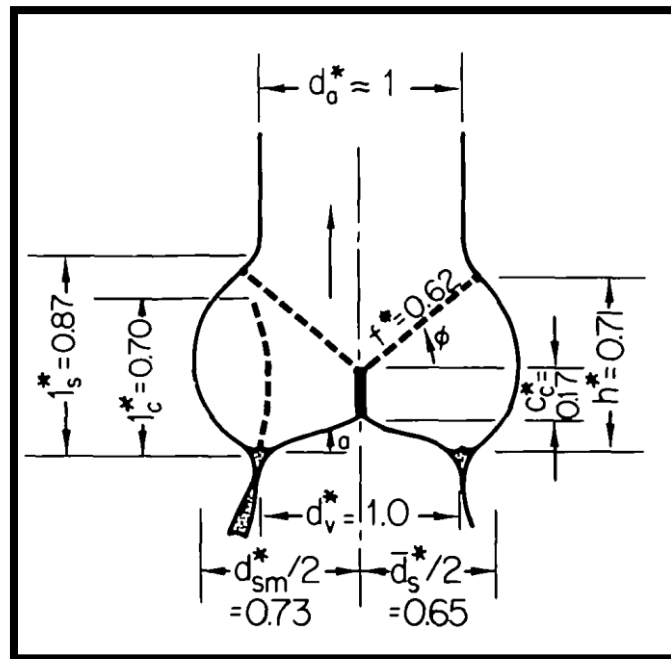


Figure 1. Mean measures (in inches) of the AV casts (Swanson & Clark, 1974).

With this model, it is likely to understand how the geometry of the AR is, so a blood flow analysis could be performed.

Furthermore, Burken, Jermihov, Vigostad & Chandran designed a three dimensional model of the AR using ANSYS software where all three Sinuses of Valsalva were constructed around idealized normal and pathological AV geometries. It is important to mention that the coronary arteries were not included, as the majority of the flow inside this structures occurs during the diastolic episode. They took values of 0.229 m for inlet diameter, 0.203 m for outer diameter of the AR study done by Swanson and Clark. Likewise, they slightly modified the dimensions of the Sinuses in order to fit different leaflet geometries which obeys the physiological principles of this cardiac structure (Burken, Jermihov, Vigmostad, & Chandran, 2011).

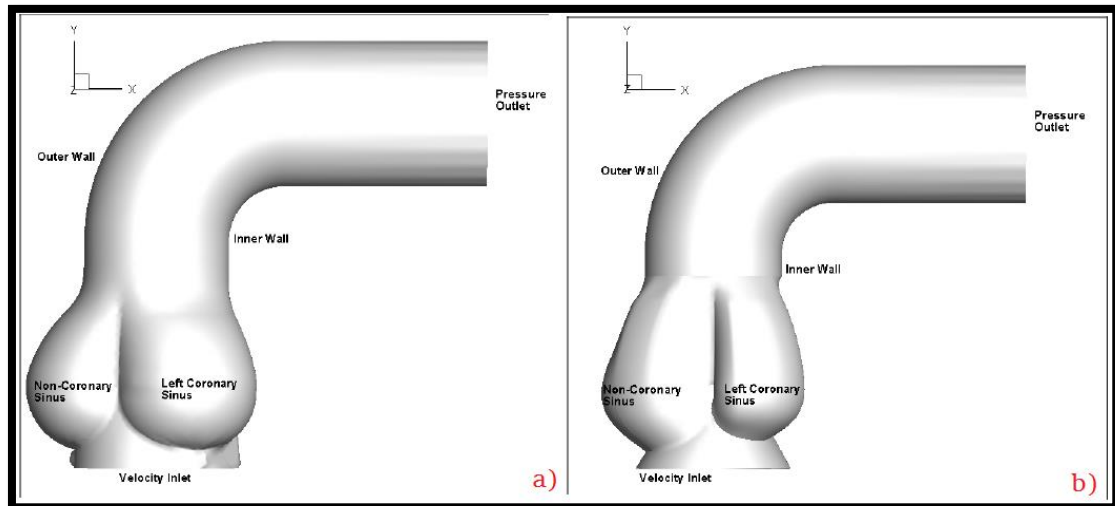


Figure 2. Two 3D different model of AR a) 5 series AR geometry b) 8 series AR geometry (Burken et al., 2011).

Opposite from the previous study, Azrul et al. used an ADINA-FSI two-dimensional model to study de deformations on the valves during systolic and diastolic periods. The reaction of the valves by the presence of the blood flow is easy-understandable as the valves present higher stresses at the side of the arterial wall where it begins, which has values of 2.6-2.3 MPa. Also, the authors mention that despite the simplicity of the geometry of the model, the computational simulations agree with medical literature observations and the model will be used in the future to determine the deformations of the valves for specific medical cases in order to take better decisions on the treatments for each patient with additional engineering background. (Azrul et al., 2011). Figure 3 shows the geometry used for this study.

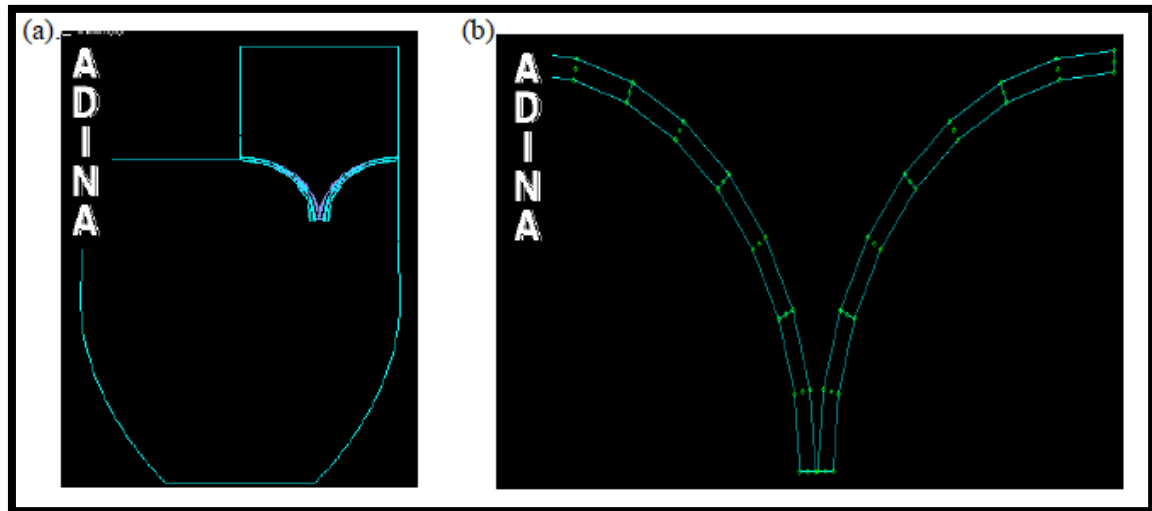


Figure 3. 2D geometry of the mitral valves used for the FSI model (Azrul et al., 2011).

2.2. Models using ALE method for FSI Analysis

The clinical performance of a valve is evaluated by both mechanical and hemodynamic characteristics (such as durability and transvalvular pressure drop). Hereafter, the interaction of the valve with the blood is essential when analyzing its functioning (De Hart, Baaijens, Peters, & Schreurs, 2003).

It is also important to remark that due to the large leaflet motions, it is difficult to adapt the fluid mesh in such a way that a proper mesh quality is maintained without changing the topology in the surface of the valves. However, previous studies show that the valve opening and closing during systole involves a strong interaction between the blood flow and the surrounding tissue. Several attempts have been made to analyze the valve behavior using numerical fluid–structure interaction models (De Hart, Peters, Schreurs, & Baaijens, 2003).

With this, the mathematical formulation of the equation of motion for a fluid is most conveniently described with respect to a Eulerian reference frame. However, this is incompatible with the Lagrangian formulation which is more appropriate to describe a

structural phase. Thus, the Arbitrary Lagrangian–Eulerian (ALE) method, combines the two different formulations and is frequently used in fluid–structure interaction analyses. Applied to the fluid phase, the ALE method requires a continuous adaptation of the fluid mesh without modification of the topology (Yeh, Grecov, & Karri, 2014). So, this authors simulated a MAV using COMSOL Multiphysics, where the pressure (normal systolic pressure of 120 mmHg) and the materials were considered as the initial conditions of the study.

Table 2. Material properties for a 2D flow study on a MAV (Yeh et al., 2014).

Property	Value	Unit
Blood Density	1060	kg/m ³
Viscosity	3.5	cP
Valve Density	2116	kg/m ³
Young's Modulus	30.5x10 ⁹	Pa
Poisson's Ratio	0.3	-

Where the model is able to closely predict the artificial leaflet dynamics, which presented a flow velocity profile from 0 – 1 m/s, applying normal cardiac pressure.

Similarly, another FSI study was made to understand the blood flow behavior in an arterial structure. In this case, the authors perform a numerical analysis of the scheme by assuming an incompressible and laminar flow using generalized Navier-Stokes system with a time-dependent module. The results show shear stress magnitudes on the wall of the artery as well as the velocity of the flow that has values near 1 m/s, which are compatible to the medical information provided in the literature. (Guerra & Tiago, 2014). An important remark of this study is the use of in COMSOL Multiphysics, which shows its versatility towards medical-engineering problems.

On the other hand, Morris et al. mention the benefits and challenges with the use of CFD in the cardiovascular medicine area. Regarding NAVs, the clinical applications

of this simulations are related to non-invasive computation and qualification of transvalvular pressure drop and regurgitant fraction for computer tomography image. (2015).

The potential clinic impact of prosthesis a real heart valves improves objective assessment and surveillance of valve disease from non-invasive imaging data. On the other hand, they remark that in the case of the valve prosthesis, “the applications are related to the optimization of its design yielding the optimal hemodynamics and low risk of design-related thrombosis and thromboembolism” (Morris et al., 2015).

Nevertheless, there are some limitations in this kind of studies. One of them is dependence upon validity of models to interpret fluid stresses in terms of hemodynamic approach. Likewise, the three-dimensional modelling of NAV and MAV requires high quality image for referencing and the computational packages are extremely heavy. However, in other to perform a simpler analysis, such as FSI two-dimensional simulations, it is vital to consider all the medical and engineering requirements and adapt them to this particular case where the heart valve opens and closes in response to the blood flow (Morris et al., 2015).

3. THEORETICAL FRAMEWORK AND MODEL DEFINITION

3.1. How the AV Works

The AV is a tricuspid valve located in the AR between the left ventricle and the aorta. Its function is to allow the path of oxygenated blood from the heart to the rest of the body by a pressure difference that allow the opening of its leaflets. This leaflets are formed by connective and smooth muscle tissue cells (Hall & Guyton, 2007).

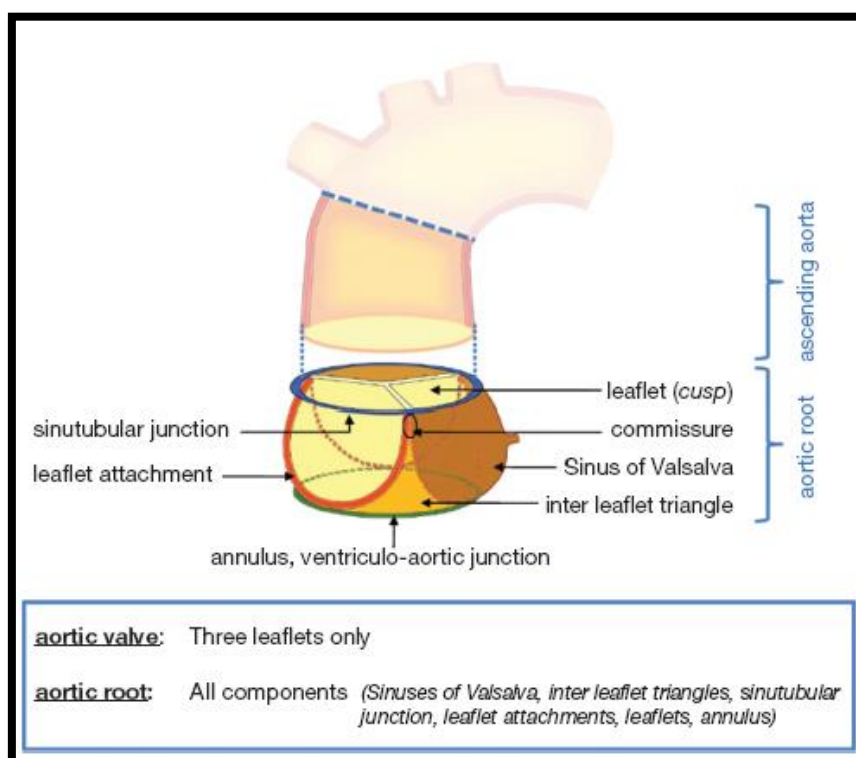


Figure 4. Anatomy of the AR (Weinberg, Schoen, & Mofrad, 2009).

The pressure difference in which the AV works is defined by the ejection period in the cardiac cycle in which the left ventricle expulses blood in the systolic episode as is showed on Figure 5 (Hall & Guyton, 2007).

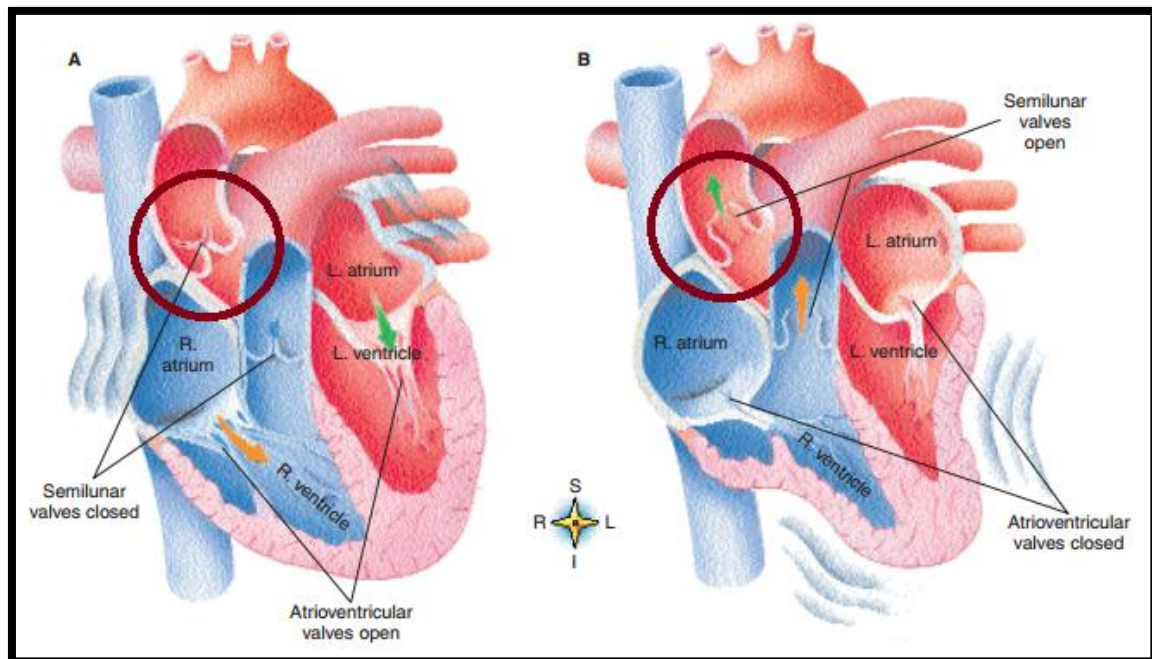


Figure 5. AV (enclosed in a circle) function inside the cardiac cycle. (A) describes the diastolic phase where the left ventricle fills with blood. (B) describes the systolic phase where the AV opens (Texas Heart Institute, 2015) .

Figure 6 shows a relationship between the volume and pressure in the cardiac cycle. Concerning our study, the period from point C to D is where the AV acts starting with an isovolumetric contraction in the left ventricle; as it is shown in the figure, the pressure gradient goes from 80 mmHg to 120 mmHg (Hall & Guyton, 2007).

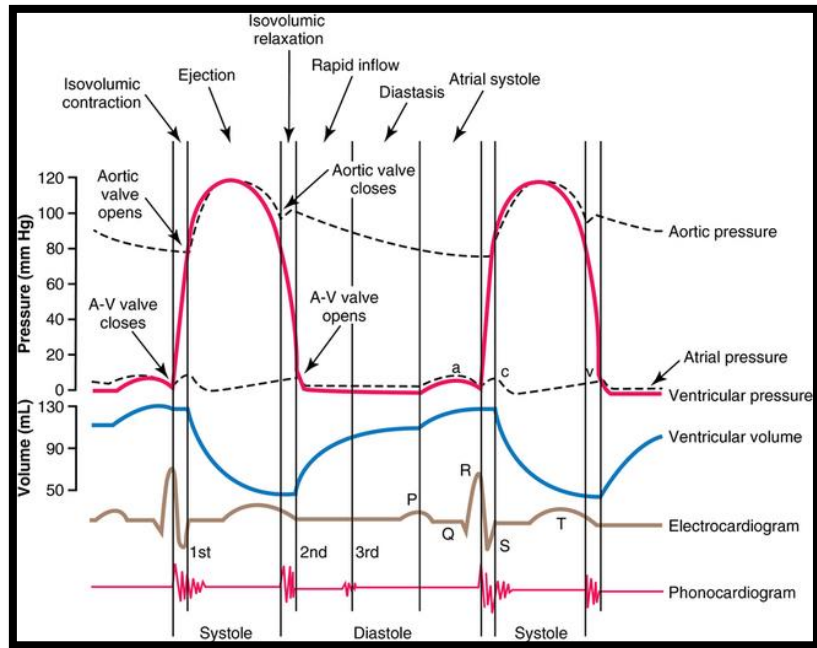


Figure 6. Cardiac cycle specifications (Hall & Guyton, 2007).

3.2. Stenosis on AV

A stenotic AV is one of the most common valvulopathies. It consists in the narrowing of the AV opening which causes a reduction on the volume of blood flow from the left ventricle to the aorta (Hall & Guyton, 2007).

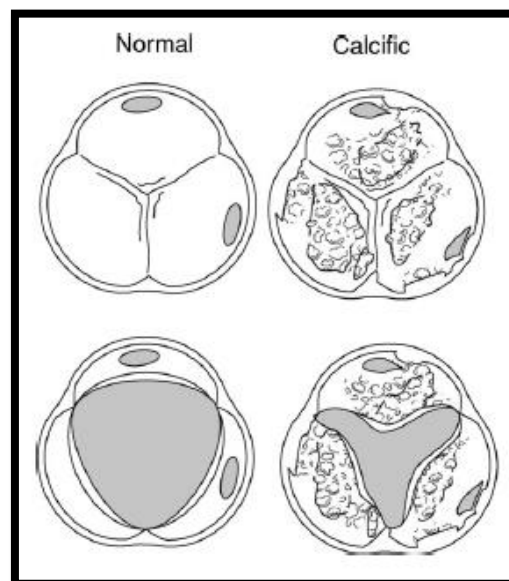


Figure 7. (Left) NAV vs (Right) moderate SAV (Baumgartner et al., 2009).

There are several types of stenosis, one of them regards the buildup of calcium deposits in the walls of the leaflets as a result of age. For this reason, calcification stenosis is more common in adults from 40 to 70 years old. It is possible that this calcific aortic stenosis would be mild, moderate and severe, depending on the growth rate of calcifications, as it is shown in Figure 8 (Weinberg et al., 2009).

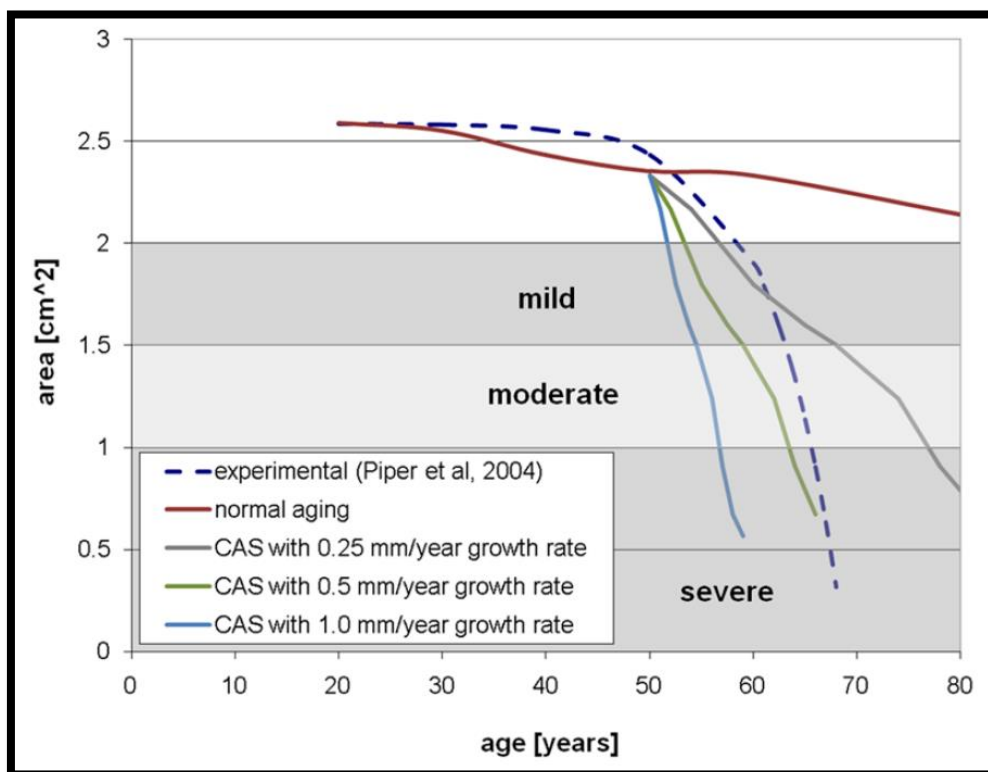


Figure 8. Effective area of blood flow in mild, moderate and severe cases of SAV (Weinberg et al., 2009).

3.3. Mechanical AV Function

In order to change an AV with a severe valvulopathy, one alternative is to perform an open heart surgery for valve replacement, in which a MAV is placed in the AR. With this prosthesis the blood flow is expected to have the same hemodynamic behavior as a NAV, with the same pressure, volume and velocity conditions. In Ecuador, St Jude

Medical is one of the authorized distributors of MAVs. One of their products is the St. Jude Medical Regent™ Mechanical Heart Valve.



Figure 9. St.Jude Medical Regent Heart Valve (St. Jude Medical, 2013).

This prosthesis consists of an orifice housing two mirror leaflets. The low profile of the prosthesis results from the bileaflet design where the pivot areas are located entirely within the orifice ring. Pivot guides located on the inner circumference of the orifice ring control the range of leaflet motion. The pivot geometry consists of arc-shaped notches at either end of each leaflet and spherical protrusions at four places on the orifice. Each leaflet rotates around two opposing spheres. In the closest position of both leaflets, the plane of each one forms a nominal angle of 25° relative to the plane of the orifice ring. In the fully open position, the plane of each leaflet forms a nominal 85° relative to the plane of the orifice ring (Zhou et al., 2016)

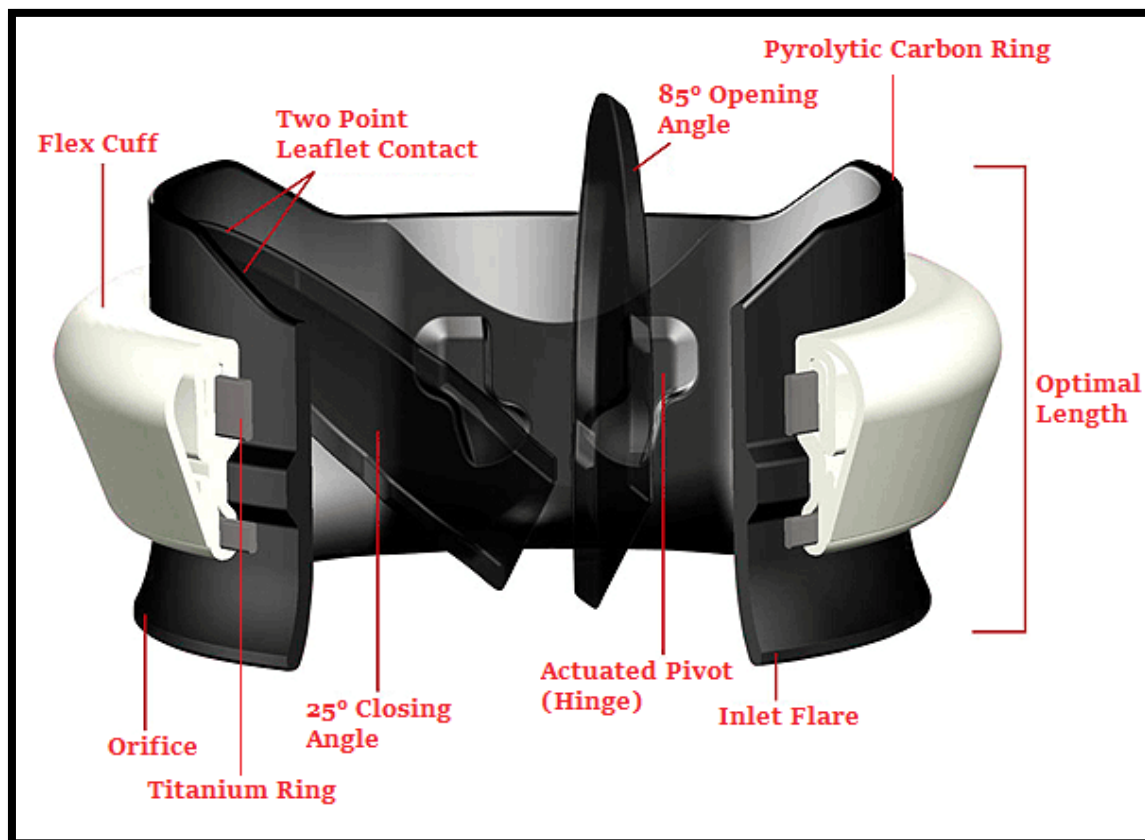


Figure 10. Parts of the MAV (St. Jude Medical, 2013).

Also, the material of this leaflets consists of pyrolytic carbon coated over a graphite substrate. The valve flex cuff is constructed of double velour polyester fabric and is mounted on the orifice using a titanium ring and secured with two titanium lock rings, as it is shown in figure 10 (ATS Medical Inc., 1999).

Also, St. Jude Medical provides sizes of this prosthesis, so it could adapt to the patient, as it is shown on table 3.

Table 3. Different St. Jude Medical MAVs regarding its size (St. Jude Medical, 2013).

N°	Tissue Annulus Diameter (mm)	Valve Orifice Inner Diameter (mm)	Geometric Orifice Area (cm ²)
1	19	17.8	2.39
2	21	19.6	2.90
3	23	21.4	3.45
4	25	23.0	4.02
5	27	24.9	4.69

From the values showed on table 3, the 4th size is going to be used in this study, since it fits the AR size of an adult male.

3.4. Theory for Fluid Interface

Navier-Stokes Equations

The fluids are prescribed by the three Navier-Stokes Equations (Comsol, 2012):

Continuity equation:

$$\frac{\delta \rho}{\delta t} + \nabla \cdot (\rho u) = 0 \quad (1)$$

This equation describes the conservation of mass.

Vector equation:

$$\rho \frac{\delta u}{\delta t} + \rho(u \cdot \nabla)u = \nabla \cdot [-pI + \tau] + F \quad (2)$$

The equation (2) pronounces the conservation of momentum.

Conservation of energy equation:

$$\rho C_p \left(\frac{\delta T}{\delta t} + (u \cdot \nabla)T \right) = -(\nabla \cdot q) + \tau : S - \frac{T}{\rho} \frac{\delta p}{\delta t} \left(\frac{\delta p}{\delta t} + (u \cdot \nabla)p \right) + Q \quad (3)$$

The equation (3) defines the conservation of energy.

It is important to keep in mind that all gases and several liquids can be considering Newtonian. In this case, the blood has a non-Newtonian behavior, but for the study, the blood can be simulated like Newtonian fluid. The viscous tensor stress, a relation that appears when the fluid is contemplate of that manner, is defined in terms of dynamic viscosity and strain rate tensor. The viscous tensor stress becomes:

$$\tau = 2\mu S - \frac{2}{3}\mu(\nabla \cdot \mu)I \quad (4)$$

Mach Number

Inside fluid dynamics, a dimensionless relation very important is the Mach number that becomes:

$$Ma = \frac{|u|}{c} \quad (5)$$

Mach number can define a flow like compressible or incompressible. This definition can change with the value of Mach number, where $Ma = 0$ represents an incompressible flow (White, 1998). This relation is important because it can affect the Navier-Stokes equations and the analysis can change. In this study, the Mach number corresponds to 3.5×10^{-3} for a velocity $u = 1.2 \frac{m}{s}$.

Incompressible Flow

Inside the fluid dynamics, the considerations of temperature are important because it can change the behavior of a gas or liquid (White, 1998) and that considerations are applied for normal conditions. This study contemplates the blood like incompressible flow. The Navier-Stokes equations considering incompressible flow becomes:

$$\rho \nabla \cdot u_{fluid} = 0 \quad (6)$$

$$\rho \frac{\partial u_{fluid}}{\partial t} + \rho(u_{fluid} \cdot \nabla)u_{fluid} = \nabla \cdot \left[-pI + \mu \left(\nabla u_{fluid} + (\nabla u_{fluid})^T \right) \right] + F \quad (7)$$

In the equations (6) and (7), the fluid velocity has been considered and the viscous tensor stress has been replaced.

Reynolds Number

This is a dimensionless relation that determine the regime of a flow. The Reynolds number establish a ratio between inertial and viscous forces (Comsol, 2012). The equation for this number allows to analyze the behavior of the inertial and viscous force. At low Reynolds number, laminar forces are surpassed for viscous forces, so the fluid tend to damp. In the other hand, at high Reynolds number, the damping inside the flow is very little. Finally, the other case is Reynolds number high enough. In this last case, the fluid present a chaotic state called turbulence. The Reynolds number become:

$$Re = \frac{\rho u L}{\mu} \quad (8)$$

3.5. Model Description

As it was mentioned before the most suitable model for this study is the FSI (Fluid-Structure Interaction) module, which analyses the behavior of a solid structure inside a fluid domain. In order to apply this model, it is important to understand several conditions inside computational simulations.

Direct Numerical Simulation Model

The chosen model to study the hemodynamics of the AVs includes a direct numerical simulation (DNS). This specializes in the analysis during the selected time step by refining the distribution of the mesh throughout the selected FSI 2D geometry. Yeh et al. perform an analysis using DNS with physiological condition in the walls of the NAV

and MAV obtaining favorable FSI results on the behavior of the valves where the blood is inside the normal parameters of its anatomy.

Fluid Structure Interaction Model

If it is desired to analyze the behavior of the AVs through the systole period, there must be a model that show accurate results around the moving boundaries of each valve, which is dependent to the hemodynamics of the system, so an FSI model is the better method to analyses this biomedical scene (Dumont, 2005).

This method is part of the CFD (Computational Fluid Dynamics) model and allows to add physics interface to model phenomena where a fluid and a deformable solid affect each other. The physics interface models both the fluid domain and the solid domain (structure) and includes a predefined condition for the interaction at the fluid-solid boundaries, in this case the NAV, SAV and MAV as structure domains inside the AR, which is the fluid domain.

Parameters for the Model

First of all, the fluid and structure conditions must be defined. Table 4 shows the characteristics of each material used in the study.

Table 4. Parameters for each material.

	Blood	Smooth and Connective Tissue (NAV)	Calcification (SAV)	Pyrolytic Carbon (MAV)
Dynamic Viscosity [Pa*s]	0.005	-	-	-
Density [kg/m³]	1060	1200	1450	2116
Young Modulus [MPa]	-	15	17.51	30500
Poisson Coefficient	-	0.37	0.35	0.3

The values for the NAV and SAV were obtained from a study that involves the analysis of anisotropic material regarding the components of connective and calcified tissue in 107 samples by tension test in axial and circumferential directions (Holzapfel, Sommer, & Regitnig, 2004). Besides, the properties of pyrolytic carbon were obtained from a simulation analysis of St Jude Medical valve prosthesis (Kwon, 2008). Finally, the blood density and dynamic viscosity were obtained from an hemodynamic reference book (Muñoz, 2000).

It is important to mention that for the cases of NAV and SAV material it is necessary to transform both parameters Young Modulus and Poisson Coefficient to first and second Lamé Parameters λ and μ , respectively. These parameters are used because is an organic material as it is recommended by Kolar (2016). The equations for this transformation are showed below.

$$\lambda = \frac{Ev}{(1 + \nu)(1 - 2\nu)} \quad (9)$$

$$\mu = \frac{E}{2(1 + \nu)} \quad (10)$$

With this, hyperelastic method could give smoother results, particularly in domains where the mesh is narrow, as a result when a solid structure has a considerable number of elasticity and great deformations, this method fits well for the study. With this, the hyperelastic smoothing method searches for a minimum of a mesh deformation energy inspired by neo-Hookean materials (Comsol, 2012).

Arterial Pressure Function

In order to simulate an accurate AR setting, so the hemodynamic computational analysis could be related to the real medical cases, the study must consider two input parameters dependent of time: arterial pressure and initial left ventricular volume.

These parameters are defined by two types of functions. They were obtained based in the data provided by figure 6 at the systolic phase. It is important to consider that this function neglects the previous diastolic phase. So, the equation for both functions are the following:

$$p_1(t) = \left(40 \sin \left(15 \frac{t}{2} \right) \right) + 80 \quad (11)$$

Equation (11) describes the arterial pressure function corresponding to the time interval from 0 to 0.36 seconds. The interval of time between 0 and 0.18 seconds is the middle of the systolic phase, in which the curve starts with a left ventricular pressure of 80 mmHg and increases to an aortic pressure of 120 mmHg. On the other hand, in the second half of the curve, the pressure drops only to 95 mmHg, approximately. The function is showed in figure 11.

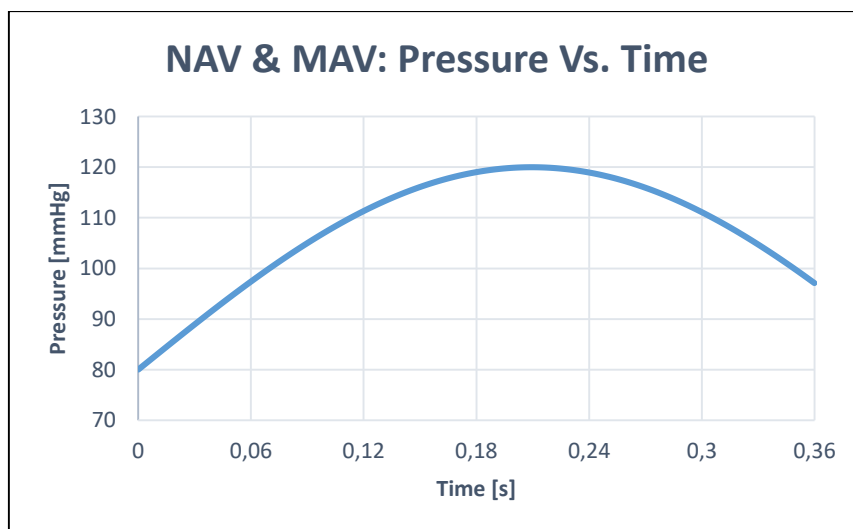


Figure 11. Normal arterial pressure function.

For the case of case of SAV, there must be another type of pressure curve obtained by the following equation:

$$p_2(t) = \left(40 \sin\left(15\frac{t}{2}\right)\right) + 70 \quad (12)$$

Equation (12) is similar to (11), with the difference that they were modified in order to fulfill a pressure from 70-110 mmHg. This rate is used to represent cardiac arrhythmias that tend to low arterial pressure depending the age of the patient, as it is showed of figure 12.

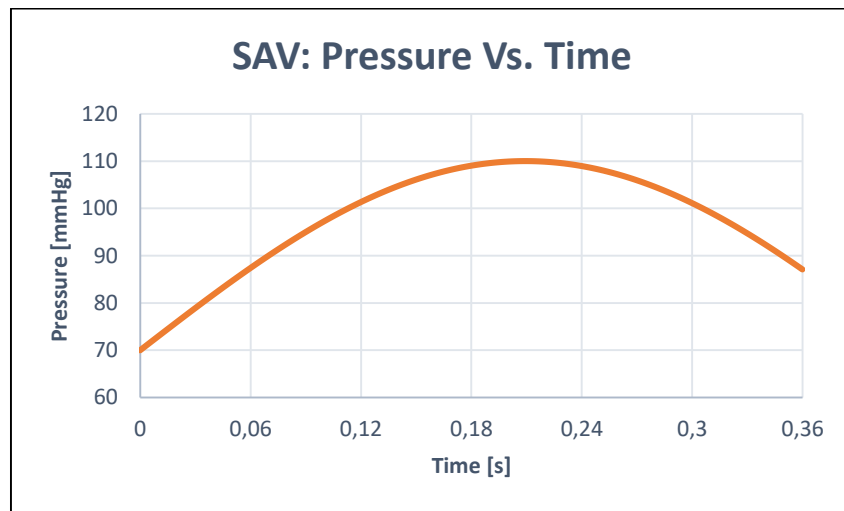


Figure 12. Arterial pressure function used for the SAV.

Initial Left Ventricular Volume

As it was mentioned before, the heart works with electrochemical conditions to create the cardiac pulse to pump blood to the body. However, for this study that electric pulse is neglected. Instead, an initial volume function is added by considering the volume values in figure 4. The function used is the following:

$$v_f(t) = 0.325\frac{t}{0.05} \quad (13)$$

In figure 13, the function expressed in equation (13) is presented. Since at systolic phase the left ventricle contracts by cardiac pulse, this volume is expelled through AR in function of the systolic time.

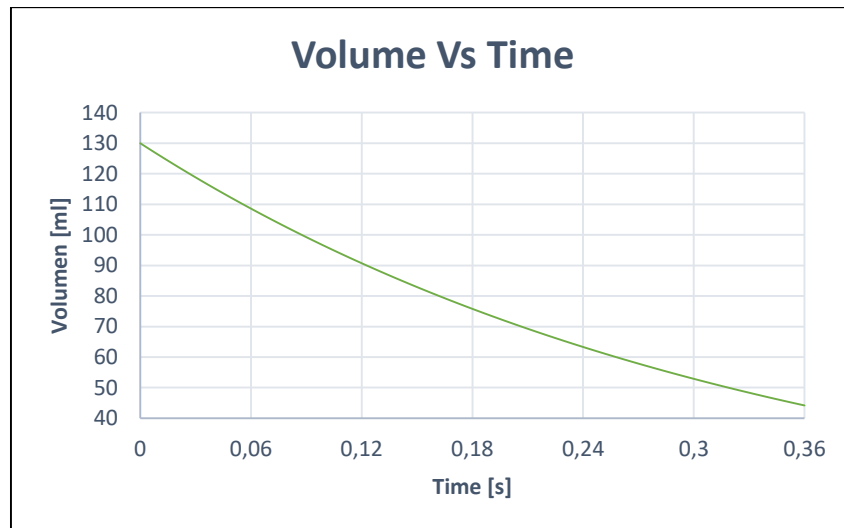


Figure 13. Initial left ventricular volume used in the study.

Geometry Specifications

As it was mention before, the study concentrates on the AR hemodynamics, so the geometry used is an approximation of this arterial section that corresponds to an adult man.

In figure 14, the geometry corresponds to the NAV geometry, which has three sections: left ventricular section, aortic root (AR), and ascending aorta. In the case of the AR, the Sinuses of Valsalva were made with quadratic Bezier curves. This applies to figure 15 and 16 too. The measures of the general geometry are exposed in table 5.

Table 5. General geometry measures.

	Left Ventricular Section	Aortic Root	Ascending Aorta
Diameter [mm]	25	41	28
Length [mm]	22	25	28

Also, the valves for the NAV and SAV were made with Bezier curves, unlike the MAV which possess straight valves. The thickness of every one of them are shown in table 6.

Table 6. Thickness of the aortic valves.

	NAV	SAV	MAV
Thickness [mm]	0.38	0.76	0.35

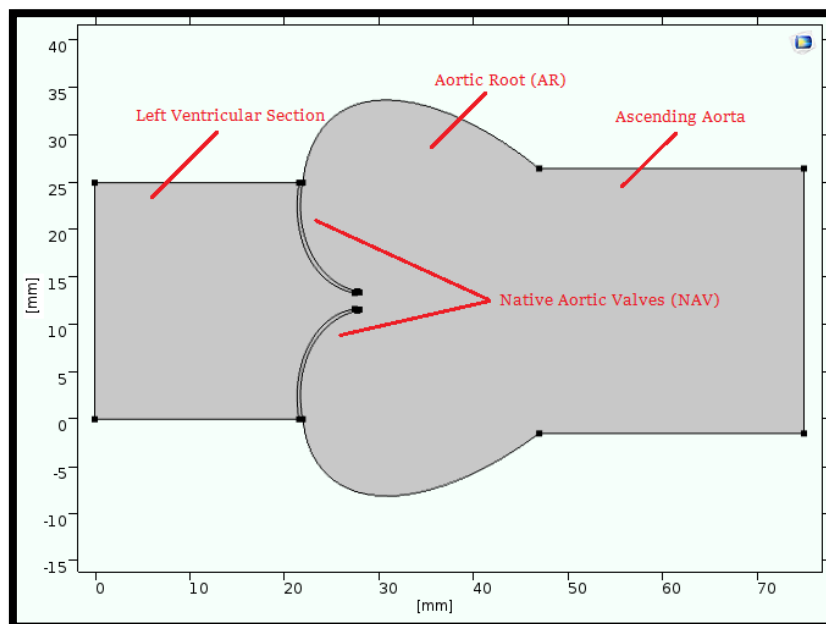


Figure 14. NAV geometry which each section described.

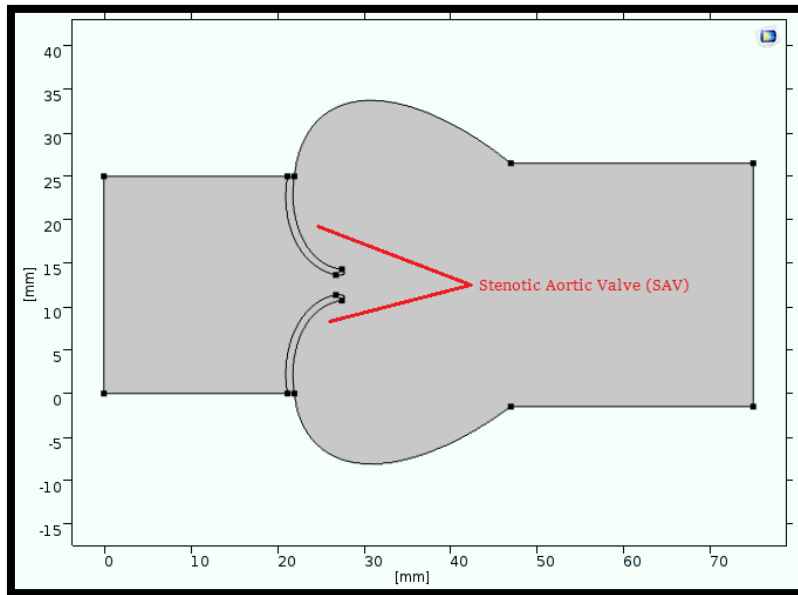


Figure 15. SAV geometry.

For figure 15, since stenosis in the AV presents an irregular structure, in order to simplify the model, the thickness for the NAV was duplicated to represent the calcifications. This characteristic together with the value of the Young Modulus and the Poisson Coefficient of table 4, helped to obtain a good approximate model for a SAV.

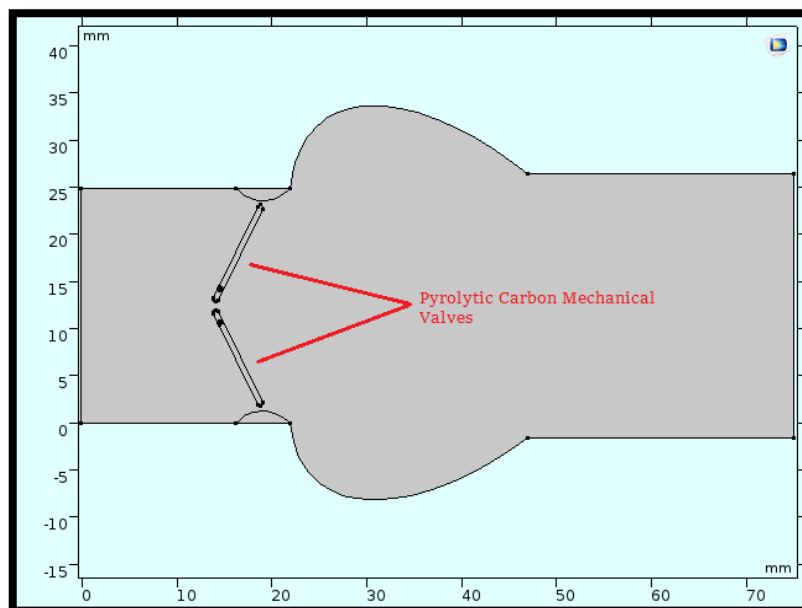


Figure 16. MAV geometry.

In the case of figure 16, the pyrolytic carbon ring located in the arterial wall had to be modeled. Its presence reduces the left ventricular section diameter to 23 mm as it is specified on table 3.

Assumptions and FSI related Conditions

To start the FSI analysis, the domains must be selected. The wall of the entire geometry is the arterial wall, which is assumed to be rigid just to simplify the analysis and concentrate the study in the blood-valve interaction. With this, the boundaries of the valve geometry are selected as a fluid-solid interface where the material is assigned depending if it is the NAV, SAV or MAV from the values of table 4. Note that the characteristics of the blood remain the same for all the cases.

Then, the inlet and outlet conditions are selected, which depends on the pressure and volume curves presented in figures 11, 12 and 13, respectively.

Now, talking about the valves from the NAV and SAV models they had assigned a fixed constraint that unites their geometry to the arterial wall. In the case of the MAV, the pivots are modeled as two fixed constraints separated 3 mm from each other obeying the valve disposition of St. Jude Medical prosthesis showed in figures 9 and 10.

Type of Mesh

For the FSI, there must be two types of meshes, one for fixed structure domain and another for the motion of the fluid. In the first one, the Lagrangian method is applied in which the mesh moves with the behavior of the structure. On the other hand, there is the Eulerian method which only concentrates in the motion of the fluid. Both combined types of meshes form the Arbitrary Lagrangian-Eulerian method, which guarantees a “higher solution accuracy due to simultaneous boundary displacement for both fluid and structure domain” (Yeh, 2011, p.50).

For this study, there has been selected three types of meshes predefined by COMSOL Multiphysics, so an error mesh analysis could be performed.

Table 7. Specifications of each mesh used for the study.

	Normal Mesh	Fine Mesh	Finer Mesh
Number of Elements	5929	8577	13856
Average Element Quality	0.9353	0.9432	0.9562
Average Grow Rate	1.312	1.277	1.225
Percentage Difference [%]	0	44.66	133.70

Table 7 shows the specifications of each mesh used in the analysis. The average element quality and the average grow rate does not present too much variation between the selected three meshes, so the possibility that divergence could occur between the results is minimal. Also, the percentage difference indicates how much the number of elements of the meshes grows in relation to the normal mesh.

To demonstrate that the three meshes are accurate on the obtaining results, figure 17 shows how the velocities behaves as a function of time, located on an arbitrary point inside the left ventricular section of the AR, which corresponds to the initial values of velocity. The graph shows that the three meshes has the same convergence behavior.

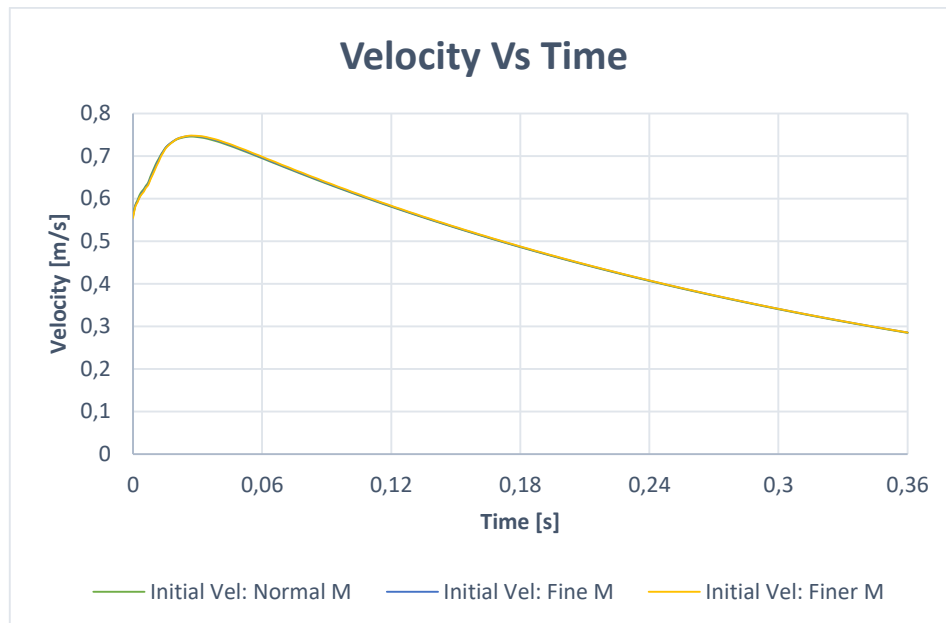


Figure 17: Comparing meshes: Initial blood velocity during the systolic phase.

Type of Study

As it was said before, this is a Time-Dependent study where the variables change over the assigned time of from 0 to 0.36 s, which corresponds to the systolic phase. Inside this study, there is a Time-Dependent solver that uses time stepping methods to obtain a synchronized solution of the problem.

Inside this Time-Dependent solver, it is assigned a Fully Coupled attribute node, which helps the simulation to compute efficiently by using a damped version of the Newton's method for finite element analysis.

4. RESULTS

The results have been separated in qualitative and quantitative analysis. For the case of qualitative results, these have been taken at the time of 0.1[s]. In the other hand, the quantitative results have been represented for all the 0 to 0.36 s interval and the values have been plotted in the same figure for the three cases of AV's. In order to improve the analysis of the results, this section has been divided to explain pressure, velocity, and Von Mises stresses behavior. Similarly, the results start with the NAV, after the SAV and finally the MAV, in that order.

4.1. Pressure

The range of values for pressure should be between 80-120 mmHg for NAV and MAV. For the case of SAV, the range of pressure should be between 70-110 mmHg. In the results of pressure, is very important to know that in the ventricular and aortic section, the curve of values should have the behavior of the physiological curves showed in figure 6. The results are as follows:

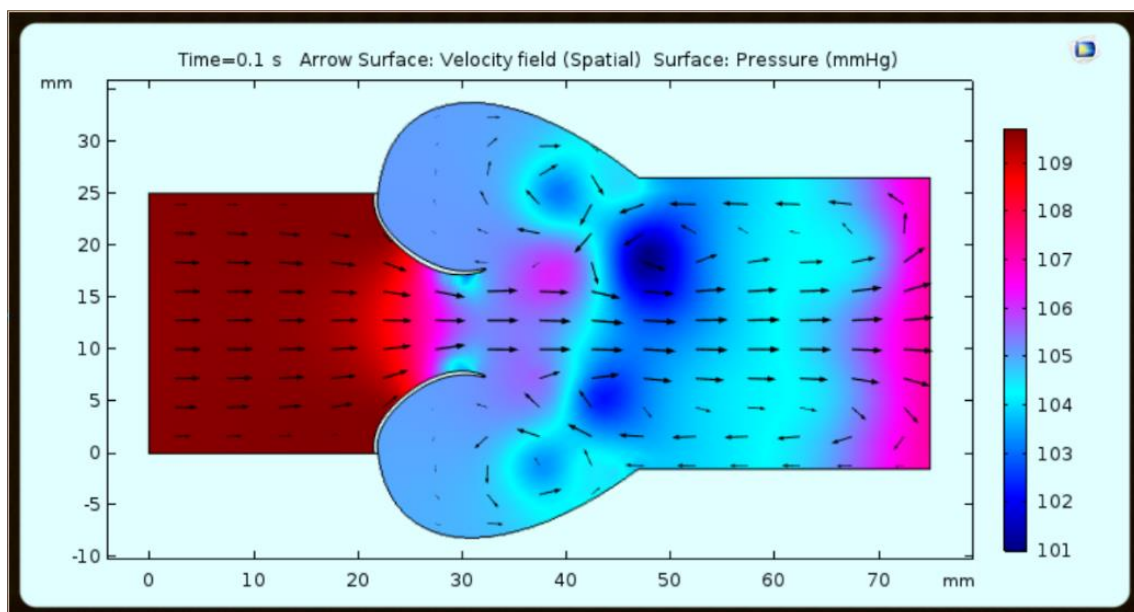


Figure 18. Pressure for NAV.

In figure 18, the range of values for pressure is between 101-109 mmHg. For the ventricular section, the pressure is very close to 109 mmHg. In the aortic section, the pressure is around of 106-107 mmHg. In figure 6, the curves of aortic and ventricular pressure correspond to the physiological curves. These curves are very similar, so in this case, the aortic pressure and ventricular pressure obtained in COMSOL are very close. The pressure difference between these curves are in magnitude of 2 mmHg. In this qualitative result for NAV, it can be appreciated some points where the pressure has different values. In these points, there have been several vortexes generations.

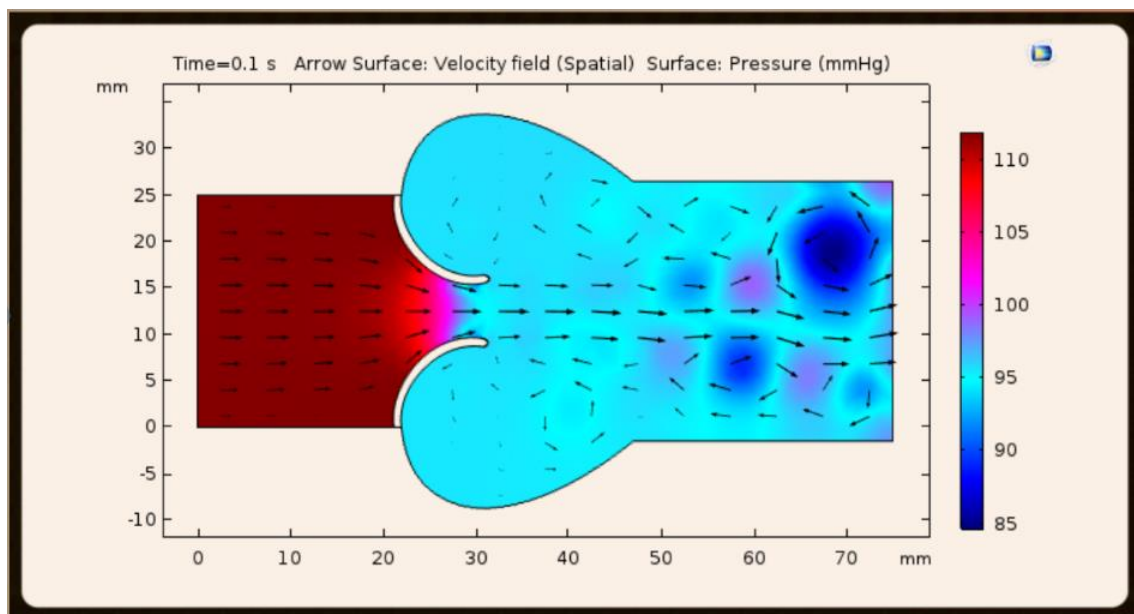


Figure 19. Pressure for SAV.

In figure 19, the range for pressure is between 85-110 mmHg. For ventricular segment in this case, the value is very close to 110 mmHg. For the aortic tract, the pressure is around 95-100 mmHg. The gradient between these sections is higher than in a NAV. For this case, the presence of vortexes at the end of aortic tract is higher than a NAV, so the values for pressure have different magnitude and the aortic pressure is not close to the ventricular pressure. In the same way, the maximum value is close to 110 mmHg and it is different to the maximum value for NAV that corresponds to 120 mmHg. The extreme

value for pressure changes in SAV because the physiological curve corresponds to a valvulopathy, thus, the range of values for pressure is different.

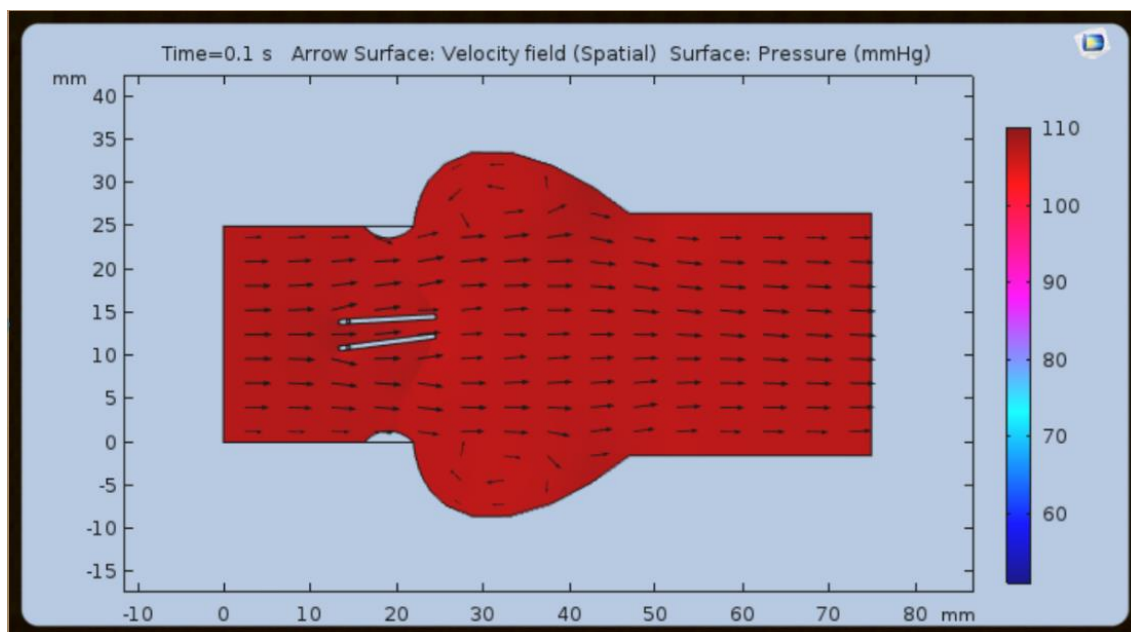


Figure 20. Pressure for MAV.

Figure 20 shows the range of values for pressure that correspond to 60-100 mmHg. Within this case, the gradient of pressure is zero because the aortic and ventricular pressure have the same value. The quantitative result displays a value approximately close to 110 mmHg in most of the geometry. It has this behavior because vortexes are not present due to the laminar flow generated after the leaflets are open. The laminar behavior is maintained because the opening efficiency of the leaflets is higher, so the vortexes are avoided and the final pressure has the behavior of the physiological curves. It is important to remember that in this case the ranges of values for physiological pressure correspond to 80-120 mmHg because the MAV has the same pressure conditions that the NAV.

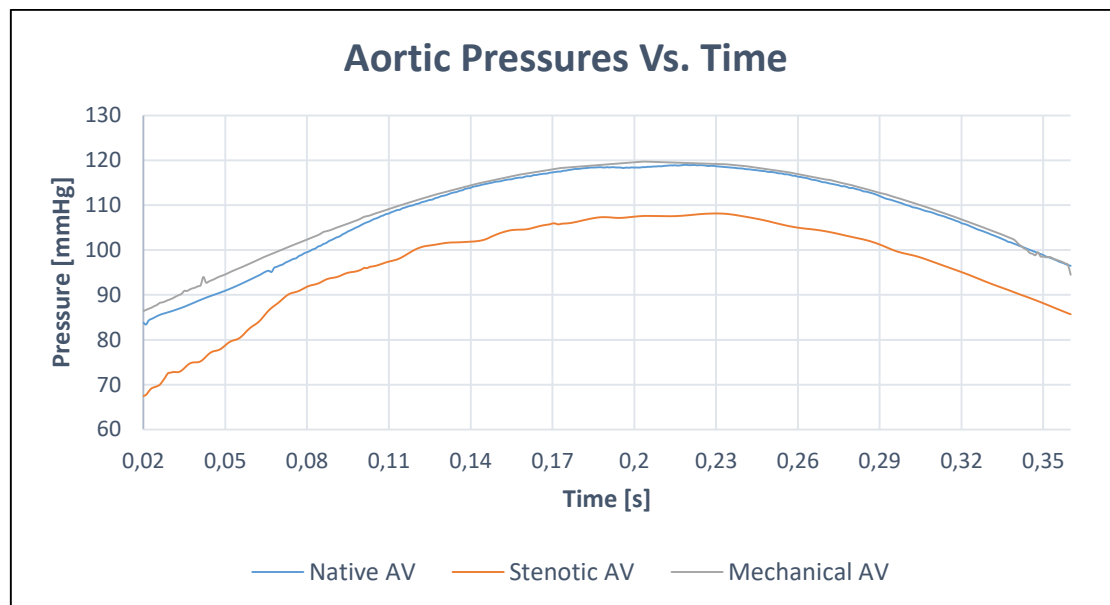


Figure 21. Quantitative results for the three cases of AV's.

Finally, figure 21 shows the curves for aortic pressure in the three cases within this study. The gray curve corresponds to MAV and its behavior is very similar to physiological curve of aortic pressure. For the case of blue curve, the values correspond to NAV, where the range of values are closer to the physiological curve like in the MAV. It is important to consider that the MAV and NAV are fulfilling the range of values 80-120 mmHg. Likewise, these two curves are higher than SAV and it has values between 70-110 mmHg. The SAV is represented by the orange curve and has the same behavior that the physiological curve, but with different range of values.

4.2. Velocity

The results for velocity have different values for each case. The magnitude of velocity depends on optimal opening area and it decreases with the elasticity of the leaflets once these are open. Likewise, the ranges of velocity for NAV and MAV must be smaller than $1.5 \left[\frac{m}{s} \right]$. The results are the following:

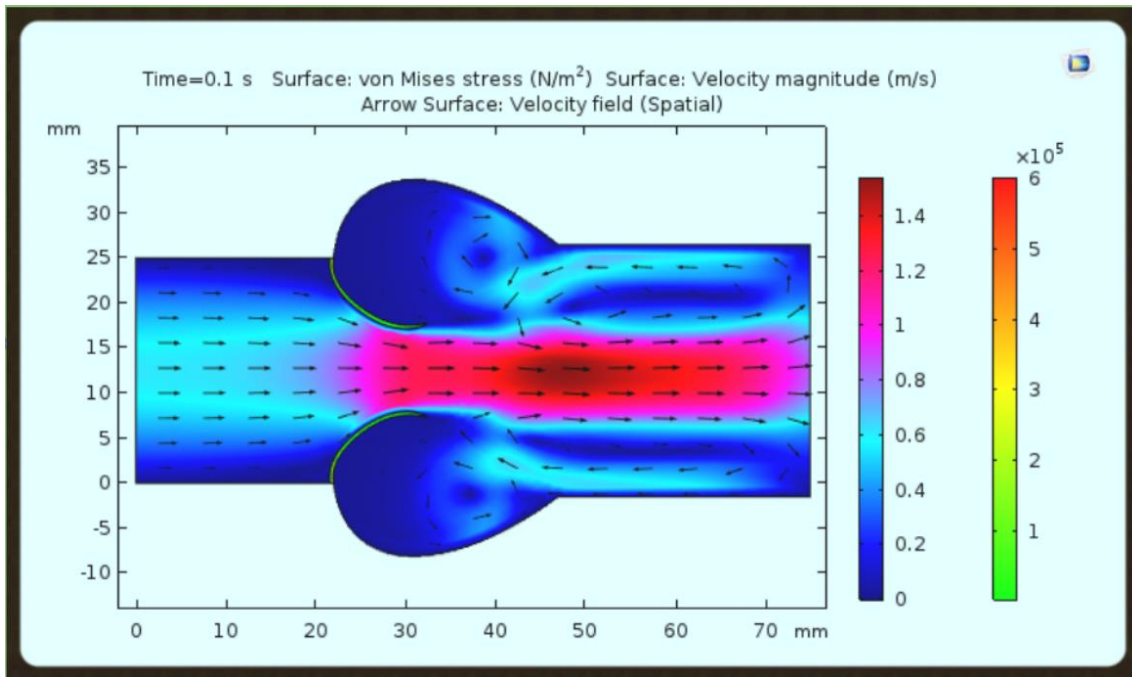


Figure 22. Velocity for NAV.

In the figure 22, the range of velocities correspond to $0-1.4 \left[\frac{m}{s} \right]$. The maximum value of velocity has been given in the optimal opening area that is the space between leaflets. The maximum value is under $1.5 \left[\frac{m}{s} \right]$, so these results are correct for NAV. Likewise, the presence of vortices is clear inside the geometry. It is important to keep in mind, that the velocity profile in the ventricular sector is parabolic because the walls has no slip condition, so the velocity of the flow is increasing from the wall to the middle of the geometry, where the value of velocity is maximum.

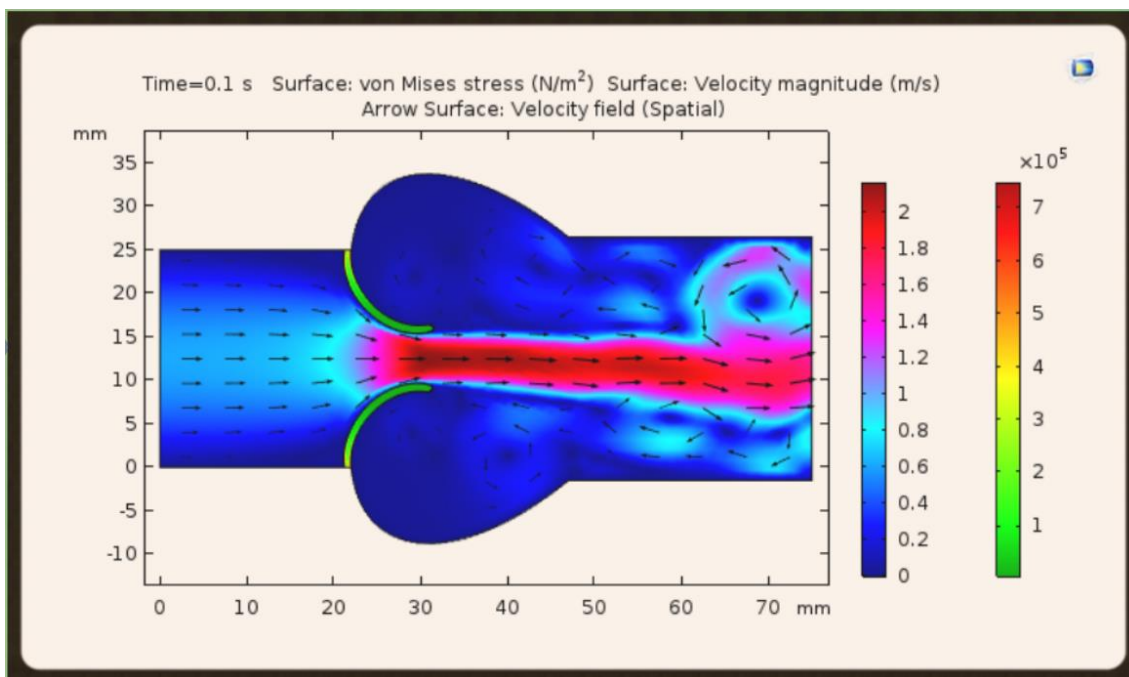


Figure 23. Velocity for SAV.

Figure 23 shows the range of velocities corresponding to $0-2\left[\frac{m}{s}\right]$. In this situation, the optimal opening area is smaller than NAV. The reduction of the optimal area is caused for the calcifications on the leaflets, consequently the elasticity decreases and its rigidity increases. According to boundary conditions, the volumetric flow is the same for the three cases, so the flow through the SAV is the same that in NAV. The velocity increases where the area decreases, therefore in SAV the reduction in the area causes that the velocity reaches higher values. In the ventricular tract, the velocity profile has a parabolic form because this case of SAV has laminar flow condition too. The maximum value for velocity corresponds to more than $2\left[\frac{m}{s}\right]$. Equally, the vortexes are higher for the SAV because the velocity is higher too.

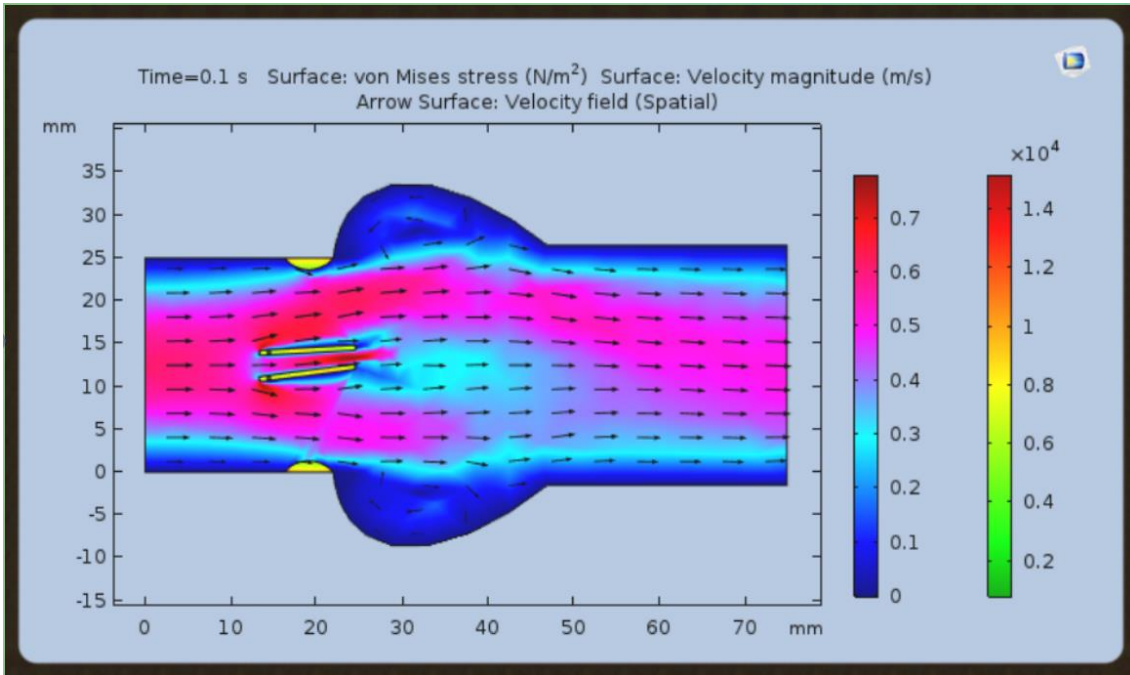


Figure 24. Velocity for MAV.

Figure 24 shows the range of velocities for SAV that correspond to $0-0.7 \left[\frac{m}{s} \right]$. For this particular case, the leaflets divide the flow in three, so the flow has more areas for the flow path. For the cases of NAV and SAV the path flow is ruled for the optimal opening area, hence the flow has only one path. The MAV has velocities lower than $1 \left[\frac{m}{s} \right]$ because the areas are bigger than the other cases of AV's. So, it is important to remember that the velocities depend on the area and for this case it is bigger, so that the velocities decreases. Also, the MAV has not presence of vortexes inside the geometry caused for the three paths that are generated for the disposition of the leaflets.

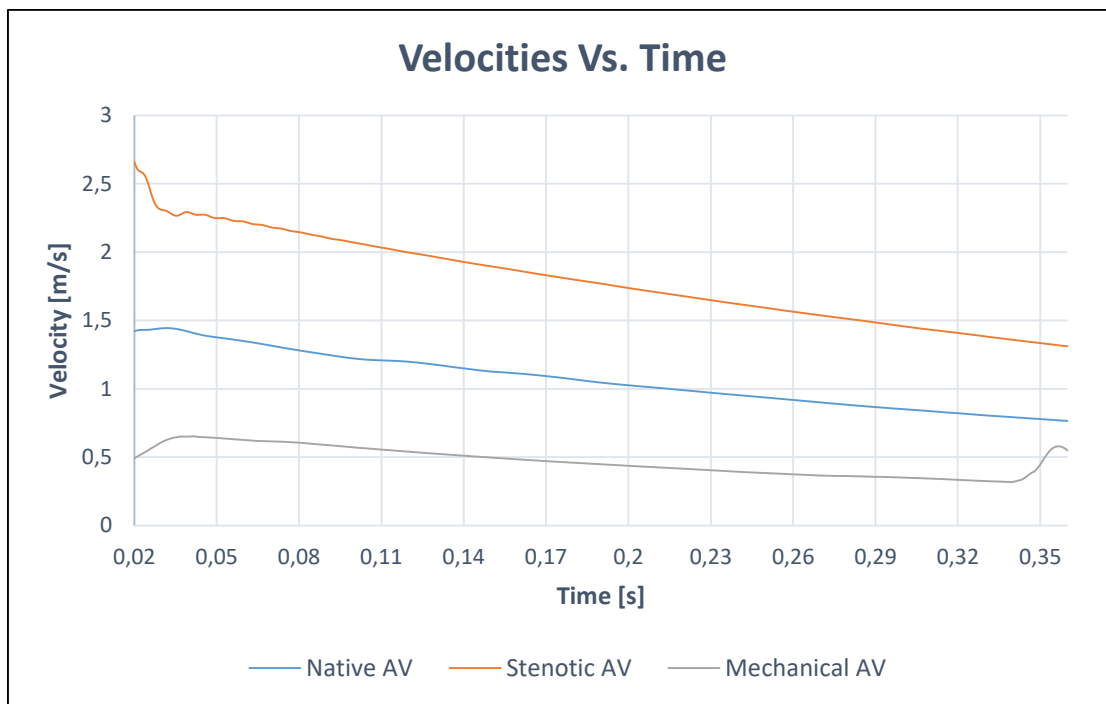


Figure 25. Velocity for AV's.

Lastly, figure 25 shows the velocity curves for the three cases analyzed in this study. The orange curve represents the velocities for SAV, where these values are higher than NAV and MAV. The leaflets for SAV have more rigidity and less elasticity caused by the calcifications. Due to the optimal opening area, which is less for the SAV, the velocity has the tendency to increase and this behavior is satisfied for all the systole. The velocities for NAV and MAV are lower than $1 \left[\frac{m}{s} \right]$ in all the time interval. The design of MAV have been created to decrease vortexes formation and improve the pass of flow, so the velocities are lower and approximately to $0.33 \left[\frac{m}{s} \right]$ that correspond to aortic velocity. It is important to remember that the higher velocities are presented in the first third because the heart sends the 70% of blood to the body in this time. The other 30% flows to the body in the other two thirds, so that the higher velocities are obtainable at the beginning of the systole.

4.3. Von Mises Stresses

The analysis for stresses has been performed only for NAV and SAV. The MAV has not been considered because its leaflets produced negligible stresses according with the material they are made. The critical point for MAV could be in the pivot, but for this study the stresses have been considered only to determine the difference between leaflets with and without calcifications. That said, the results are as follows:

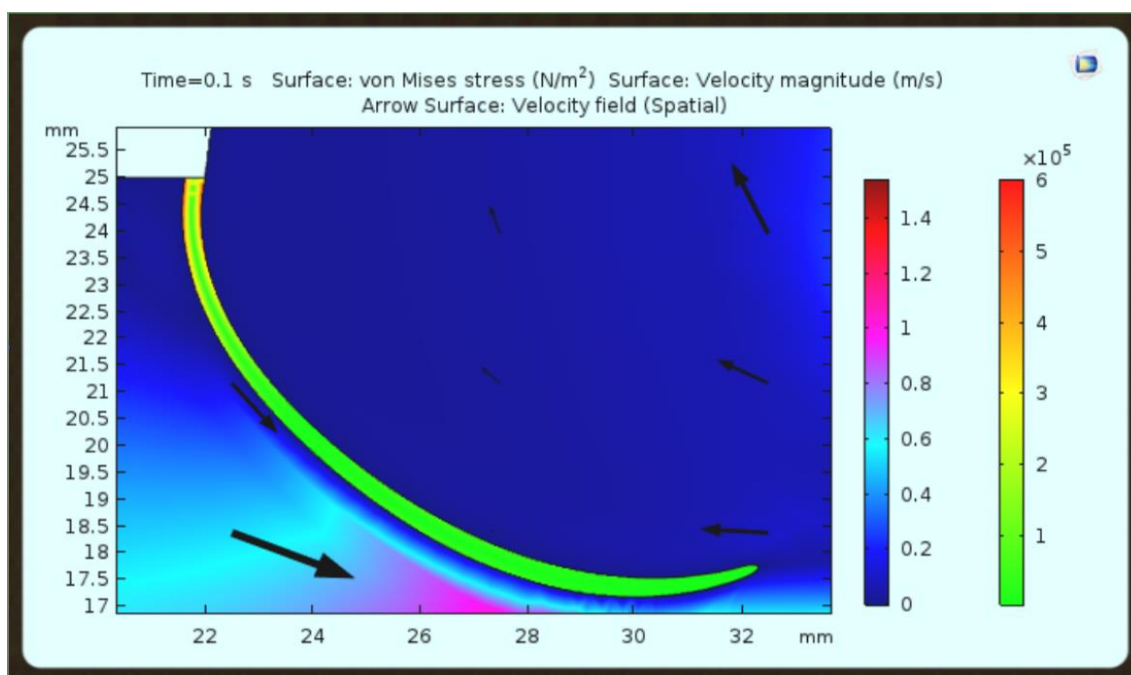


Figure 26. Von Mises stresses for NAV.

Figure 26 shows the Von Mises stresses for NAV and the range of values are between 0.1-0.6 [MPa]. The interior face (concave side) of AV's is in compression and the external face (convex side) is in tension. The leaflets for NAV have less thickness and the Young Modulus is less than SAV. The critical points for the leaflets are in the surroundings among leaflets and aortic wall. The behavior of the leaflets in that position corresponds to cantilever beam, where the leaflets have flexion due to passage flow.

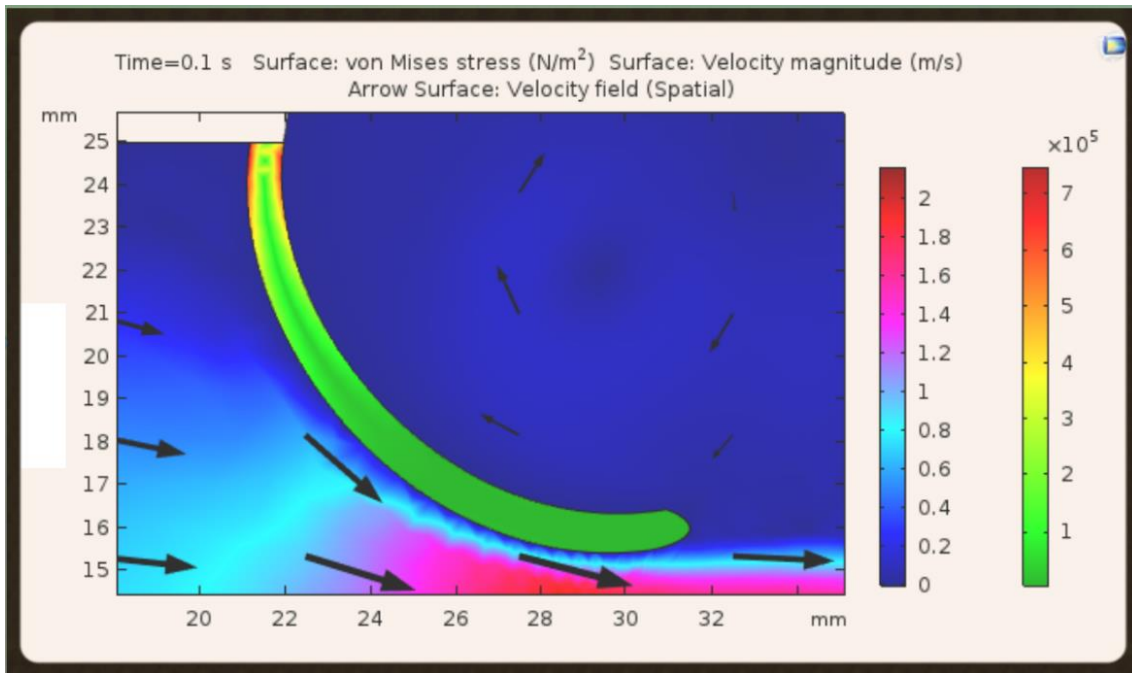


Figure 27. Von Mises stresses for SAV.

Figure 27 shows the Von Mises stresses for SAV with range of values between 0.1-0.7 [MPa]. In this case, the stresses are higher than NAV because the leaflets have more rigidity due to calcifications. In the same way, the interior face (concave side) is in compression and the external face (convex side) is in tension. The leaflets for SAV have more thickness, so that the displacement is lower than in a NAV.

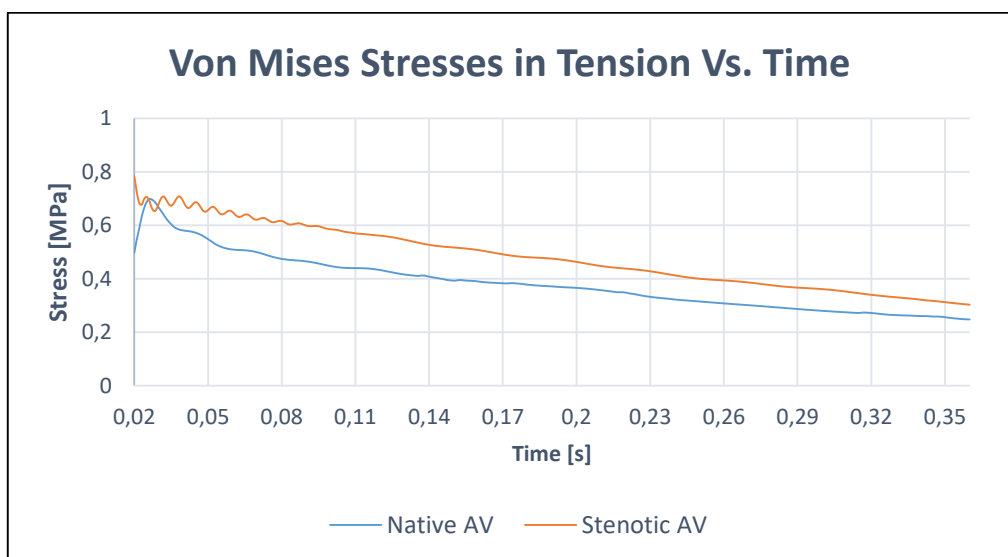


Figure 28. Von Mises stresses in tension for AV's.

Figure 28 displays the quantitative results for NAV and SAV. The values for Von Mises stresses are higher in all the time interval for tension that correspond to the convex side.

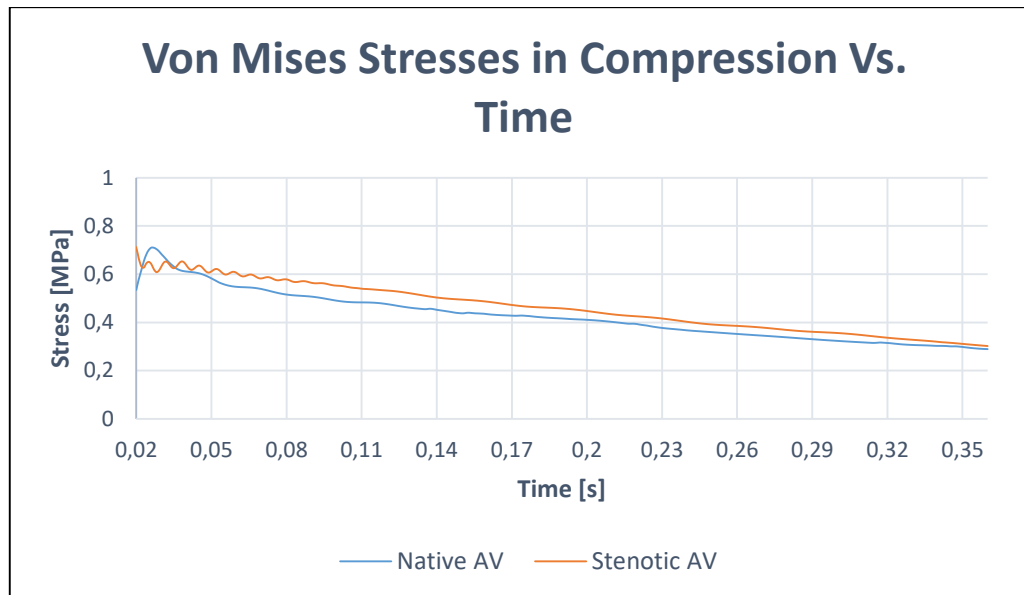


Figure 29. Von Mises stresses in compression for AV's.

Finally, figure 29 shows the values for Von Mises stresses in compression for NAV and SAV. Likewise, the values for SAV are higher than NAV and it is important to remember that it is caused due to calcifications in the leaflets. For this case, the values for compression are lower than tension and that results are due to the flow path, since the flow direction is from ventricular tract to aortic tract.

5. CONCLUSIONS

The study was carried out by the software COMSOL Multyphysics and it allowed to contribute with information about hemodynamic behavior in AVs in Ecuador. Inside this, the study was simulated with FSI module that permitted a better coupling between flow and structure; in this case among leaflets and blood. The module FSI allowed to improve the convergence to obtain the results. The study was governed by the equations of Navier –Stokes for a 2D fluid model and it allowed to understand the hemodynamics difference between NAV, SAV, and MAV. In the same way, the study allowed to obtain values for pressures, velocities, and Von Mises stresses.

For the pressures, it was possible to determine the curves inside the geometry due to the blood passage. This study was approximated to the real model because the physiological curves for aortic pressure and ventricular volume were established like boundary conditions. Similarly, the properties were assigned for flow and mechanical structure; in this case the leaflets. Also, the time simulation was computed in the time interval of a systole that corresponds to 0.36[s]. The curves for pressure were similar to physiological curves that correspond to a range between 80-120 mmHg for NAV and MAV; for the MAV the range was 70-110 mmHg.

For the velocities, the study allowed to find the range of values for the three cases of VA´s. Inside the velocities, the maximum value was found in SAV due to the optimal opening area is lower than NAV caused for calcifications in the leaflets. For NAV and MAV the values for velocities are lower than $1.5 \left[\frac{m}{s} \right]$, so that the ranges of velocities that were found are correct, supported by the literature data. The range of velocities for SAV allowed to determine that the case of stenosis is moderate because is approximately the double of the range for NAV.

For the Von Mises stresses the range of values were higher for SAV and lower for NAV; for tension and compression. The Von Mises stresses in tension were higher than compression due to the flow path, since the flow direction is from ventricular tract to aortic tract. As a final point, this study showed that it is possible to approach medical engineering problems until the point of demonstrating that the medical engineering simulations are the future to solve problems and find solutions with less time, cost and good precision.

6. RECOMMENDATIONS

Before starting this study, is very important to have basic knowledge about physiology and anatomy. As a result, in this study the medical terms should be known and the properties of the leaflets and geometry should be similar, that recommendation should be very significant to keep in mind. In the same way, it is important to have knowledge about COMSOL Multiphysics because it allows to take advantage of the versatility of the software and improves the simulations to get better results that are very close to the reality. To conclude, the last recommendation is about computational resources. The time of simulations is very big and these depend of the machine that have been selected to carry out the study. It is important to have good computational resources that allow to get results in a short time with excellent precision.

7. FUTURE WORK

This study can be improved if this is carried out between different careers, for example biology and medicine. The union with other careers could improve the solution of the problem because it allows to analyze it from different perspectives, so in the study it will be possible to implement other properties for the material and flow. By the same token, this study can go further with implementation of an application that can determine a simulation to study the hemodynamic behavior of the blood through of AV's where the variables of the problem change with the patient, for example aortic pressure, ventricular and aortic diameter, cardiac frequency, etc. Nowadays, does not exist a union between simulations and medical analysis, so the research in this field could improve and create this bond. To close, the future work could also focus in mechanical design because the MAV needs an improvement regarding its material, since the implantation of a pyrolytic carbon MAV requires that the patient take anticoagulant medicine for the rest of his/her life. So the implementation of a 100% anticoagulation material different from the pyrolytic carbon used in this study could be an advanced improvement that deserves further investigation.

8. REFERENCES

- Aguirre, M., & A, L. (2015). Distribución de las Principales Cardiopatías del Adulto en el Noroccidente del Ecuador. *Revista Ecuatoriana de Cardiología*, 1(1), 1.
- Aguirre, M., Ortega, H., & Arcos, R. (2015). Estadística del Manejo Quirúrgico, Posquirúrgico y Mortalidad Pos-Cirugía Cardíaca: A Propósito del Primer Año de Funcionamiento de la Unidad de Cuidados Posoperatorios de Cirugía Cardíaca. *Revista Ecuatoriana de Cardiología*, 1(1), 1.
- ATS Medical Inc. (1999). ATS open pivot bileaflet heart valve. Minneapolis, USA: ATS Medical.
- Azrul, M., Mohd, H., Osman, K., Hazreen, N., Hasni, M., & Maskon, O. (2011). Computational Simulation of Heart Valve Leaflet under Systole Condition using Fluid Structure Interaction Model. *International Conference on Environment and BioScience*, 21, 6–10.
- Baumgartner, H., Hung, J., Bermejo, J., Chambers, J. B., Evangelista, A., Griffin, B. P., ... Quiñones, M. (2009). Echocardiographic assessment of valve stenosis: EAE/ASE recommendations for clinical practice. *European Journal of Echocardiography*, 10(1), 1–25. <https://doi.org/10.1093/ejechocard/jen303>
- Burken, J., Jermihov, P., Vigmostad, S. C., & Chandran, K. B. (2011). Determining the Effect of Congenital Bicuspid Aortic Valves on Aortic Dissection Using Computational Fluid Dynamics, 8, 2011.
- Comsol. (2012). Comsol Multiphysics User's Guide. *The Heat Transfer Branch*, 709–745, The Heat Transfer Branch. [https://doi.org/10.1016/S0260-8774\(99\)00111-9](https://doi.org/10.1016/S0260-8774(99)00111-9)
- De Hart, J., Baaijens, F. P. T., Peters, G. W. M., & Schreurs, P. J. G. (2003). A computational fluid-structure interaction analysis of a fiber-reinforced stentless aortic valve. *Journal of Biomechanics*, 36(5), 699–712. [https://doi.org/10.1016/S0021-9290\(02\)00448-7](https://doi.org/10.1016/S0021-9290(02)00448-7)
- De Hart, J., Peters, G. W. M., Schreurs, P. J. G., & Baaijens, F. P. T. (2003). A three-dimensional computational analysis of fluid-structure interaction in the aortic valve. *Journal of Biomechanics*, 36(1), 103–112. [https://doi.org/10.1016/S0021-9290\(02\)00244-0](https://doi.org/10.1016/S0021-9290(02)00244-0)
- Dumont, I. K. (2005). Experimental and numerical modeling of heart valve dynamics. <https://doi.org/N/A>
- Guerra, T., & Tiago, J. (2014). Improving Blood Flow Simulations Using Known Data. *COMSOL Conference in Cambridge*, (1). Retrieved from <https://www.comsol.com/paper/improving-blood-flow-simulations-using-known-data-18417>
- Hall, J. E., & Guyton, A. C. (2007). *Tratado de Fisiología Médica* (12da Edici). Jackson, Mississippi: Elsevier Saunders.
- Hasan, A., Ragaert, K., Swieszkowski, W., Selimovic, S., Paul, A., Camci-Unal, G., ... Khademhosseini, A. (2014). Biomechanical properties of native and tissue engineered heart valve constructs. *J Biomech*, 47(9), 1949–1963. <https://doi.org/10.1016/j.jbiomech.2013.09.023>

- Holzappel, G. A., Sommer, G., & Regitnig, P. (2004). Anisotropic mechanical properties of tissue components in human atherosclerotic plaques. *J Biomech Eng*, 126(5), 657–665. <https://doi.org/10.1115/1.1800557>
- Kolar, P. (2016). *Heart Valve Mathematical Models*. Rochester Institute of Technology.
- Kwon, Y. J. (2008). Structural analysis of a bileaflet mechanical heart valve prosthesis with curved leaflet. *Journal of Mechanical Science and Technology*, 22(11), 2038–2047. <https://doi.org/10.1007/s12206-008-0621-4>
- Morris, P. D., Narracott, A., von Tengg-Kobligk, H., Silva Soto, D. A., Hsiao, S., Lungu, A., ... Gunn, J. P. (2015). Computational fluid dynamics modelling in cardiovascular medicine. *Heart (British Cardiac Society)*, heartjnl-2015-308044-. <https://doi.org/10.1136/heartjnl-2015-308044>
- Muñoz, E. (2000). *El océano interior – Leyes físicas de la hemodinámica* (1ra Edicio). Mexico: Instituto Politécnico Nacional.
- St. Jude Medical. (2013). Regent™ Mechanical Heart Valve FlexCuff™, (May 2012), 5833.
- Swanson, W. M., & Clark, R. E. (1974). Dimensions and Geometric Relationships of the Human Aortic Value as a Function of Pressure. *Circulation Research*, 35(6), 871–882. <https://doi.org/10.1161/01.RES.35.6.871>
- Texas Heart Institute. (2015). *Anatomy of the Cardiovascular System*. Retrieved from http://www.texasheart.org/HIC/Anatomy/images/fig1_crosslg.jpg
- Weinberg, E. J., Schoen, F. J., & Mofrad, M. R. K. (2009). A computational model of aging and calcification in the aortic heart valve. *PLoS ONE*, 4(6), 1–10. <https://doi.org/10.1371/journal.pone.0005960>
- White, F. (1998). *Fluid Mechanics*. (J. Holman & J. Lloyd, Eds.) (4th Editio). Rhode Island, USA: McGraw-Hill.
- Yeh, H. H. (2011). *Computational Analysis of Fluid Structure Interaction in Artificial Heart Valves*. University of British Columbia.
- Yeh, H. H., Grecov, D., & Karri, S. (2014). Computational modelling of bileaflet mechanical valves using fluid-structure interaction approach. *Journal of Medical and Biological Engineering*, 34(5), 482–486. <https://doi.org/10.5405/jmbe.1699>
- Zhou, F., Cui, Y. Y., Wu, L. L., Yang, J., Liu, L., Maitz, M. F., ... Huang, N. (2016). Analysis of flow field in mechanical aortic bileaflet heart valves using finite volume method. *J Med Biol Eng, M*. <https://doi.org/10.1007/s40846-016-0106-3>